1994 WHITEHEAD MEMORIAL LECTURE

Physics and Chemistry of Partial Discharge and Corona

Recent Advances and Future Challenges

R. J. Van Brunt

National Institute of Standards and Technology,
Gaithersburg, MD

ABSTRACT

Results of recent research on physical and chemical processes in partial discharge (PD) phenomena are reviewed. The terminology used to specify different types or modes of PD are discussed in light of a general theory of electrical discharges. The limitations and assumptions inherent to present theoretical models are examined. The influence of memory propagation effects in controlling the stochastic behavior of PD is shown. Examples of experimental results are presented that demonstrate the nonstationary characteristics of PD which can be related to permanent or quasi-permanent discharge-induced modifications (aging) of the site where the PD occur. Recommendations for future research are proposed.

1. INTRODUCTION

WITHIN the past fifteen years there has been a rapid growth of research activity concerned with partial discharge (PD) phenomena. A PD is generally thought of as a highly localized or confined electrical discharge within an insulating medium between two conductors, and in some cases PD is the precursor to a complete electrical breakdown or fault. The occurrence of PD can be the cause of electrically-induced aging of insulating materials manifested, for example, by formation of corrosive gaseous byproducts, erosion, sputtering, and 'tree' formation. PD, despite its localized nature, is an enormously complex phenomenon that often exhibits chaotic, nonstationary, or fractal type behavior with seemingly unpredictable transitions between different modes that exhibit distinctly different time-dependent characteristics. The existence of many different observed modes of PD behavior has caused some confusion and inconsistencies in the terminology used to define these modes, and this has, in turn, led to attempts at clarifying the terminology [1]. One source of confusion in the search for generalized descriptors of PD phenomena arises from the infinite variety of geometrical and material conditions under which PD can occur.

The recent upsurge of research on PD phenomena has been driven in part by development of new fast digital and computer-based techniques that can process and analyze signals derived from PD measurements [2]. There seems to be an expectation that, with sufficiently sophisticated digital processing techniques, it should be possible not only to gain new insight into the physical and chemical basis of PD phenomena, but also to define PD

1070-9878/94/$3.00

'patterns' that can be used for identifying the characteristics of the insulation 'defects' at which the observed PD occur. Among the various digital techniques that have been applied recently to PD measurements are

1. precise pulse-shape and pulse-burst characterizations using broad-band detection [3–5],
2. recording of phase-resolved PD pulse-height distributions using various types of digitizers or multichannel analyzers [6–8],
3. quantification of PD pulse-to-pulse or phase-to-phase memory propagation effects using stochastic analysis [9, 10], and
4. removal or reduction of noise using digital filtering techniques [11].

The impressive results from use of these measurement techniques have been compared with predictions from computer simulations, *e.g.*, of discharge pulse shape [4, 12] and stochastic behavior [13, 14].

In addition to the introduction of new signal processing techniques applied to PD measurement, recent investigations have been undertaken also into effects that PD have on the properties of the materials in which they occur. Included in these investigations are measurements of

1. gaseous byproducts from the discharge [15, 16],
2. removal of solid material or other local changes in morphology [17],
3. changes in solid dielectric surface resistivity [18, 19],
4. surface acidification, oxidation or deposition of material [20–22], and
5. growth of voids, cracks, or trees within a dielectric [23–26].

It has been noted [18, 27] that the PD-induced changes in the physical and chemical characteristics of the discharge site will in turn cause changes in the PD behavior that make the phenomenon inherently nonstationary. The susceptibility to nonstationary behavior complicates the interpretation of PD signals. In general, PD phenomena are described theoretically by a set of coupled nonlinear differential equations from which it can be shown that feedback and memory effects are important and can be responsible for complex stochastic behavior. The problems of quantifying, unraveling, interpreting, and understanding the complicated behavior of PD are the challenges of present and future research.

PD has been the subject of numerous published reviews [1, 28–32] some of which were presented in previous Whitehead Memorial Lectures [33–35]. The focus of the present review will be on relatively recent work published within the past fifteen years dealing primarily with the basic physical and chemical processes responsible for, or associated with the discharge phenomenon. Particular emphasis will be given to work carried out in our laboratory on PD in SF_6, and SF_6/O_2 gas mixtures in point-plane or point-dielectric barrier gaps.

2. DEFINITIONS AND TERMINOLOGY

A persistent difficulty that has plagued the field of gas-discharge physics is that of imprecision and confusion in the terms used to define different types of electrical-discharge phenomena. There continues to be disagreement about the meaning and appropriateness of the words that have been applied as designators of discharge type. The definitions used for PD phenomena have been discussed in recently published papers [1, 4, 28]. As has been noted in these works, part of the difficulty with finding precise definitions is a consequence of the multitude of different types of discharge behavior that have been observed. Another issue confronting those who seek meaningful definitions is that concerning the regions of transition between different types of discharge behavior. An example is the case of the transition from a pulsating negative corona (Trichel pulse [36]) to a glow discussed in the work of Cernak and Hosokawa [37]. A Trichel pulse can be viewed as a discharge current pulse associated with a transient glow discharge or as a glow discharge that tries to develop but is extinguished by accumulating space charge.

The purpose of this Section is to clarify the meaning of the terms used here to designate discharge phenomena. It is not intended as a recommendation to standardize definitions. It should always be kept in mind that different words are sometimes used to identify what are in reality simply different modes or manifestations of the same phenomenon. One is confronted with a situation that is not unlike that of describing the phenomena of weather. It is easy to distinguish 'clear' or 'cloudy' days but 'partly cloudy' or 'mostly sunny' days present a problem of imprecision in definition.

As will be discussed in Section 3, PD phenomena can be described in general by a set of coupled differential equations, and different discharge types may simply correspond to different solutions of these equations for different boundary conditions. Ideally the 'mathematical description' provides the only meaningful 'definition'. In practice, because of the complexity of a complete mathematical treatment, one is forced to rely on qualitative descriptors that cannot have precise definitions.

The term 'partial discharge' will refer here to a class of discharge phenomena that satisfy a set of restrictions on such parameters as size, intensity, and temperature. Included in the category of PD are various types of discharges that have been given different names such as corona, constricted glows, electron avalanches, localized

Table 1. Table of Symbols

N	gas number density (cm^{-3})	Q_a	attachment cross section (cm^2)
N_e	electron number density (cm^{-3})	Q_M	momentum transfer cross section (cm^2)
N_p	positive ion number density (cm^{-3})	k_{ij}	reaction rate coefficient (cm^3/s)
N_n	negative ion number density (cm^{-3})	q_n	amplitude of n^{th} PD pulse (C)
α	ionized coefficient (cm^{-1})	Δt_{n-1}	time separation between n^{th} and $(n-1)^{th}$ pulses
η	electron attachment coefficient (cm^{-1})	q_{lim}	limiting maximum corona pulse amplitude (C)
β_1	electron–ion recombination coefficient (cm^3/s)	$p_o(q_n)$	unconditional PD pulse amplitude distribution
β_2	ion-ion recombination coefficient (cm^3/s)	$p_1(q_n\|\Delta t_{n-1})$	conditional PD amplitude
D_p, D_n	ion diffusion coefficients (cm^2/s)	Δt_l	ion transit time in gap (s)
e	electron charge (C)	Z_d	gap spacing (cm)
ϵ_o	permittivity of free space	$Q^{\pm}$	integrated pos. or neg. PD charge (C)
ϵ_i	dielectric permittivity ($i = 1, 2$)	ϕ_i^-	phase of i^{th} neg. PD pulse (rad)
σ	surface charge density (C/cm^2)	$p_o(Q^{\pm})$	unconditional integrated charge distribution
Γ	surface conductivity (A/Vcm)	$p_o Q^{\pm}$	unconditional integrated charge distribution
$\vec{K}$	surface current density (A/cm^2)	$p_o(\phi_i^-)$	unconditional phase distribution
E	electric field strength (V/cm)	$p_o(\phi_i^-\|Q^+)$	conditional phase distribution
$\vec{E}_t$	transverse electric field component (V/cm)	$R_e^{\pm}$	rates of electron release(s^{-1})
λ_e	electron mean free path (cm^{-1})	$w^{\pm}$	surface work functions (eV)
$\vec{v_e}$	electron velocity (cm/s)	ω	frequency of applied voltage (rad/s)
ε	electron kinetic energy (eV)	I_d	corona discharge current (A)
m_e	electron mass (kg)	$[X]$	concentration of chemical species X (mol)
γ_{ph}	efficiency factor (electrons/photon)	ΔE_s	space charge contribution to local field ($V\ cm^{-1}$)
ν	photon frequency (s^{-1})	μ	ion mobility (cm^2/Vs)
f	electron energy distribution function	$r(X)$	normalized production rates (mol/C/SF_6 mol)
F	electron energy distribution function	r_t	sum of normalized production rates (mol/C/SF_6 mol)
Q_i	ionization cross section (cm^2)		

discharges. PD is assumed here to be a gas discharge that may or may not occur in the presence of a solid (or liquid) dielectric. The presence of the solid (or liquid) dielectric can affect the behavior of PD by providing a source of secondary electrons or by modifying the local field due to accumulation of surface or bulk charge.

The actual discharge zone of PD is assumed to be restricted to a portion of the insulating gap between two conductors to which voltage is applied. The discharge zone is defined here to be that region in which the electric-field strength is sufficiently high to allow release of electrons by various collision processes either in the gas or on a surface. The examples considered here are mainly restricted to PD generated in point-to-plane type electrode gaps where the plane electrode may or may not be covered by a dielectric surface. The discharge zone in this case is confined to the immediate vicinity of the point electrode. Although, there may exist regions outside of the discharge zone in which charge transport occurs, they are not considered to be part of this zone because the field strength is not high enough to support ionization. On the other hand, the existence of charge carriers outside of the discharge zone can have an influence on activity within this zone.

PD is also assumed to be a relatively 'cold discharge' in the sense that the mean energy of electrons is always

considerably higher than the mean energy of the molecules in the gas, *i.e.*, the discharge is not very effective in heating its surroundings, and there is a lack of equilibrium between charged and neutral species.

The term 'corona' applies to a special category of PD that occur in cases where solid insulating surfaces are absent or are far removed from the discharge zone. The designations of positive and negative to corona refer to the polarity of the voltage applied to the most highly stressed electrode assuming that this can be defined. In the case of a point-plane gap, the point is obviously the most highly stressed electrode. In the case of a point-point gap, the polarity designation losses its meaning. In general, the behavior of positive and negative corona can be quite different and can exhibit distinctly different modes. For example, regular Trichel pulse corona [36] occurs only at a negatively stressed point electrode. The differences between positive and negative corona discharge behavior are, in part, a consequence of the different predominant sources of initiatory or secondary electrons [28, 38].

PD can exhibit either pulsating or nonpulsating characteristics. The pulsating behavior generally results from the buildup of surface charge or space charge at the discharge site which causes the local electric-field strength to drop below the level necessary to sustain ionization. The pulsating PD are said to be self-quenching. Pulsating behavior is particularly common when PD occur in proximity to a solid insulating surface, *e.g.*, in a dielectric cavity or in a point-dielectric gap. Pulsating discharges that occur in gaps in which one or both of the electrodes is covered with a dielectric surface are sometimes referred to as dielectric barrier discharges or silent discharges [39].

A particular type of nonpulsating discharge that will be considered in the present work is a glow discharge. Glow discharges are sometimes designated as either positive or negative depending on whether they occur near the anode or cathode. The specific type of glow discharge considered in this work is a constricted negative glow corona that occurs near a negatively stressed point electrode. In electronegative gases like air and SF_6, this type of glow is preceded at lower gap voltages by the pulsating (Trichel-pulse) corona mentioned above. It is constricted in the sense that the region of ionization and light emission (discharge zone) is confined to the immediate vicinity of the point electrode.

Glow discharges can occur under a wide range of conditions and can exhibit different voltage-current and time-dependent behavior. At the present time, there seems to some confusion and disageement about the proper definitions and terminology that should be applied to this type of discharge [1, 2, 19, 40–42]. The present discussion will be restricted to steady glows for which the spatial and temporal characteristics are determined largely by an equilibrated ion-electron space-charge density distribution that significantly modifies the electric field within the discharge zone. The glow is 'steady' in the sense that, for a given applied voltage, the discharge current is constant or changes very slowly with time. In general, 'glow discharges' can be unstable, especially near conditions identified with transitions to other modes, and can exhibit fluctuating, oscillatory, or pulsating behavior [43, 44]. The different observed modes of glow-type discharge behavior have been described using a variety of terms such as 'abnormal glow', 'pulsating glow', 'pseudoglow', and 'swarming microdischarge'. The meanings of these terms will not be explored here.

There is a weaker class of discharges that is often placed in the category of PD, namely electron avalanches and diffuse Townsend discharges. These discharges are 'weak' in the sense that their development is not significantly affected by space charge, *i.e.*, the electron and ion densities are not high enough to perturb the applied electric field. An electron avalanche is an electron multiplication process that is usually very localized in its development and appears as a pulse. Its growth is usually restricted by geometrical constraints, and its pulsating behavior is mainly due to an inability to regenerate, *i.e.*, its intensity as measured in terms of number of ions produced and radiation emitted is too weak to produce a sufficient number of secondary initiatory electrons needed for regeneration. An electron avalanche can be considered as a special case of a Townsend discharge which may also be diffuse, *i.e.*, it can occur over a relatively broad area between parallel plates, and can be regenerative, *i.e.*, self-sustained. The electron-avalanche or Townsend discharge descriptions are applicable to the early stages of breakdown or PD development when the numbers of electrons and ions are relatively low. When the local space-charge density reaches a level high enough to significantly perturb the local field, the discharge can propagate in the gas by the streamer mechanism discussed in earlier works [28, 35]. It is generally believed that photoionization accounts for the high speed of streamer propagation [45, 46]. Under some conditions, pulsating PD may involve streamer formation in the development stage of the discharge.

Most of the PD phenomena considered here, as well as those of most practical interest, are self-sustained, *i.e.*, their maintenance does not require exposure of the gap to external radiation. Discharges known as sparks, arcs, or flashover are considered to be complete electrical breakdown processes that are too intense or too hot to be categorized as PD. There are some authors [40, 41], however, who include intermittent or self-quenching sparks among PD phenomena.

3. GENERAL THEORY OF PARTIAL DISCHARGE

PD phenomena can be described mathematically by a set of coupled differential equations. A solution to these equations, if it can be found, will yield observable characteristics of the discharge such as the time dependence of the discharge current. It can be argued that all types of discharges such as glow-type corona or diffuse Townsend discharges satisfy the same set of equations. The differences in discharge type should arise from differences in assumed initial conditions (defined, for example, by gas content, pressure, and dielectric surface conductivity), and assumed boundary conditions (defined, for example, by electrode geometry, thickness of a dielectric, and applied voltage). In general, the discharge model should include both physical and chemical processes. Examples of physical processes are: ionization by various mechanisms, electron attachment, diffusion of neutral and charged species, and deposition or sputtering at surfaces. In the category of chemical processes are various chemical reactions that can occur in the gas phase or on surfaces and may involve neutral or charged species. In general, the physical and chemical processes cannot be treated as independent, *e.g.*, the rate of ion formation by electron collision affects the rate of reactions between ion and neutral molecules that may be responsible for formation of observable stable or quasi-stable molecular byproducts.

The coupling between various types of discharge processes is illustrated by the block diagrams in Figure 1. The normal physical processes that affect the initiation, growth, and extinction of a discharge are indicated in Figure 1(a), and physical and chemical processes associated with discharge-induced 'aging' are indicated in Figure 1(b). Aging processes involve modifications of gas composition and electrode or dielectric surface conditions and generally have a much longer time frame than the processes responsible for development of a single discharge event. Advantage can be taken of this large difference in time scales to simplify discharge models that consider both the discharge physics and related discharge chemistry [39, 45, 46].

An example of a set of coupled equations similar to that used by Morrow [12, 47] to model negative-corona pulses in oxygen is given below. These equations include only the physical processes occurring in the discharge, *i.e.*, they correspond to the situation shown in Figure 1(a). In a somewhat generalized version of Morrow's corona model, the electron, positive ion, and negative ion densities are assumed to satisfy the continuity equations

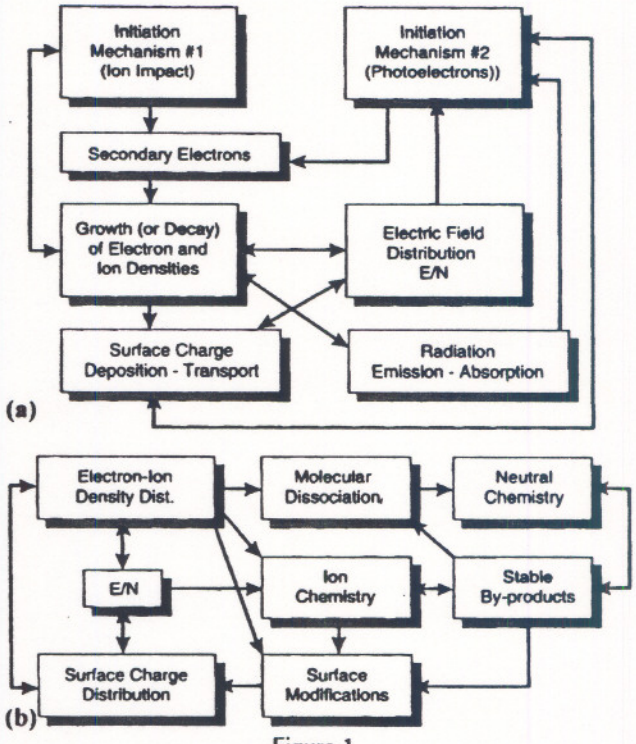

Figure 1.

(a) Block diagram of a model for discharge initiation, growth, and decay that applies in a short time frame in which PD-induced aging can be neglected. (b) Block diagram of a discharge model that includes physical and chemical changes due to PD-induced aging that applies in a long time frame.

$$\frac{\partial N_e}{\partial t} = N_e\alpha|\vec{v}_e| - N_e\eta|\vec{v}_e| - N_eN_p\beta_1 - \nabla\cdot(\vec{v}_eN_e) + \nabla^2(D_eN_e) \tag{1}$$

$$\frac{\partial N_p}{\partial t} = N_e\alpha|\vec{v}_e| - N_eN_p\beta_1 - N_nN_p\beta_2 - \nabla\cdot(\vec{v}_pN_p) + \nabla^2(D_pN_p) \tag{2}$$

$$\frac{\partial N_n}{\partial t} = N_e\eta|\vec{v}_e| - N_nN_p\beta_2 - \nabla\cdot(\vec{v}_nN_n) + \nabla^2(D_nN_n) \tag{3}$$

Here N_e, N_p, and N_n are respectively the electron, positive-ion, and negative-ion number densities and v_e, v_p, and v_n are the corresponding electron, positive-ion, and negative-ion drift velocities. In general, the densities and drift velocities depend on position in the gap. The parameters α, η, and β_1, are respectively the electron-impact ionization, attachment, and electron-ion recombination coefficients which also depend on position. The positive and negative ion diffusion coefficients and ion-ion

recombination coefficients are denoted by D_p, D_n, and β_2 respectively. The spatial variations of the above coefficients are determined primarily by their dependence on the local electric field-to-gas density ratio, $E(\vec{r})/N$, where N, without a subscript, denotes the neutral gas density, generally assumed for PD conditions to be much greater than the charged-particle densities. The vector $\vec{r}$ denotes position in the discharge gap measured from an arbitrary origin.

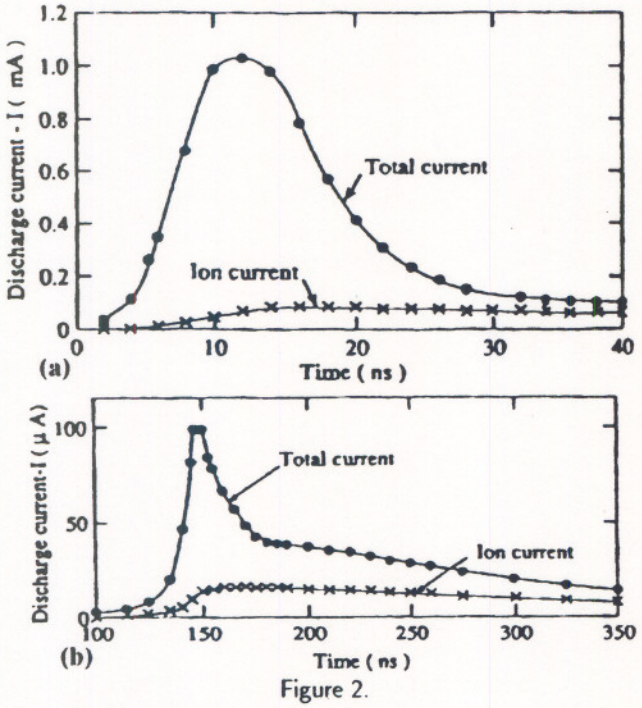

Figure 2.

Calculated PD current pulses for a 0.5 mm gap in an air-like gas mixture at atmosperic pressure for: (a) high overvoltage and (b) low overvoltage [4].

Equations (1) to (3) are coupled to the three-dimensional Poisson's equation for the electric field

$$\nabla \cdot \vec{E}(\vec{r}) = \frac{e}{\epsilon_o}[N_p(\vec{r}) - N_n(\vec{r}) - N_e(\vec{r})] \qquad (4)$$

where e is the electron charge, and ϵ_o is the permittivity of free space, which is assumed to apply in the gas. If it can be assumed that ionization, attachment, recombination, and diffusion are the only significant processes, then the electrical characteristics of the discharge can be modeled by numerically solving the above set of simultaneous equations subject to boundary conditions that apply, for example, at the electrode or dielectric surfaces [12, 50]. By using a model based on the above equations, Morrow was able to predict the shape of the first negative-corona pulse in oxygen [12, 49]. Similar models have been used to calculate PD pulse shapes for small gaps or gaps in which solid dielectrics are present [4, 50]. Lui and Raju [51] have recently developed a Monte-Carlo method to simulate corona current pulses in SF_6. Figure 2 shows examples of PD current pulses calculated by Novak and Bartnikas [4] for a 0.5 mm gap in a model gas (air-like mixture) for high and low overvoltages. Indicated in this Figure are the total current and the ion current component. The calculations are consistent with observations [4, 52, 53] which show that the electron component of PD pulses typically have a fast rise time and a width that is less than 50 ns. It is also seen from the example shown in Figure 2 that details of the pulse shape can depend significantly on the conditions of the gap in which the PD is formed.

When solid dielectrics are present, the surface boundary conditions can be quite complex and may exhibit a spatial and temporal dependence. The electric field at a dielectric boundary depends on the instantaneous surface charge density σ according to the requirement [50, 54]

$$[\epsilon_2 \vec{E}_-(\vec{r}', t) - \epsilon_1 \vec{E}_+(\vec{r}', t)] \cdot \vec{n} = \sigma(\vec{r}', t) \qquad (5)$$

where $\vec{n}$ is a unit vector normal to the surface and ϵ_2, ϵ_1 and $\vec{E}_-, \vec{E}_+$ are the corresponding permittivities and fields that apply on either side of the boundary. The value of σ at any time is determined by the fluxes of charged particles (ions and electrons) at the surface, by the probabilities that ions either stick to the surface or are reflected, and by the probability that charged particles are ejected from the surface by ion bombardment or other mechanisms.

Assuming that the bulk conductivity of the dielectric is much less than its surface conductivity Γ, it is necessary from charge conservation that the surface charge density satisfy a continuity equation of the form

$$\nabla \cdot \vec{K} + \frac{\partial \sigma}{\partial t} = s \qquad (6)$$

where $\vec{K}$ is the surface current density and s is a source term. Assuming that Γ is independent of the field, the surface current density is related to the tangential component of the electric-field strength $\vec{E}_t$ at the surface by

$$\vec{K} = \Gamma \vec{E}_t \qquad (7)$$

which gives

$$\vec{E}_t \cdot \nabla \Gamma + \Gamma \nabla \cdot \vec{E}_t + \frac{\partial \sigma}{\partial t} - s = 0 \qquad (8)$$

allowing that Γ can depend on $\vec{r}'$. In the absence of the source term, the solution to Equation (8) leads to a local decay of the charge density [55, 56]. In general, the source term depends on the incident ion flux, which can, in turn, depend on the field at the surface, e.g., at a sufficiently high charge density, the incoming ions can simply

be repelled from the surface. The dynamics of surface charging when a dielectric is present, as represented by Equation (8), must be considered in a complete model of PD.

Both dielectric and metallic surfaces in the discharge gap are sources and sinks for charged particles. Secondary processes for release of electrons at surfaces by ion or photon bombardment, quenching of metastable excited species, or field emission are important in initiating and sustaining PD. Under conditions of high electrical stress, such as near a sharp point electrode, the secondary processes may depend on the local electric-field strength. If we consider only the release of photo-electrons from a cathode, the derivative $\partial N_e/\partial t$ within approximately one mean-free path λ_e of an area element dA of the cathode surface will be given by

$$\frac{\partial N_e}{\partial t} \simeq \frac{1}{\lambda_e}\sum_{\nu}\gamma_{ph}(\nu, dA)\Phi(\nu, dA, t) - \nabla\cdot(\bar{v}_e N_e) \quad (9)$$

where Φ is the time-dependent photon flux (number of photons per second per unit area) at dA for a photon of frequency ν, γ_{ph} is the efficiency factor (number of photoelectrons released per incident photon), and $\bar{v}_e$ is the mean photoelectron velocity. In general, γ_{ph} can depend on the location of dA, *i.e.*, the properties of the cathode surface need not be uniform. On a longer time scale, γ_{ph} can have a time dependence due to discharge-induced aging effects. The flux Φ must be computed from radiation transport theory that takes into account the electron-impact excitation coefficients, absorption coefficients, and cascading effects [12].

Equations (1) to (3) are valid only if the coefficients α, η, and β_i are constants that are independent of time and depend only on the local reduced field strength E/N. In general, a complete description of the electron transport in a discharge requires the determination of the phase-space distribution function $f(\vec{v}_e, \vec{r}, t)$, which can be found either from a solution of the Boltzmann transport equation [57]

$$\frac{\partial f}{\partial t} + \vec{v}_e\cdot\nabla f + \frac{e}{m_e}\vec{E}\cdot\nabla_v f = I(f) \quad (10)$$

or from a Monte-Carlo simulation [58]. In Equation (10), m_e is the electron mass and $I(f)$ is a source-sink term, usually referred to as the collision integral. This term accounts for the transport of particles into and out of a volume of phase space due to collisions. The transport equation is essentially a continuity equation in phase space, and various numerical methods have been developed to solve this equation [59–61] under different conditions.

For conditions of steady-state and spatial uniformity of the field where

$$\frac{\partial f}{\partial t} = 0 \qquad \nabla f = 0 \quad (11)$$

the solution of Equation (10) yields a field-dependent velocity distribution function that can be converted to an electron kinetic-energy distribution function $F(\varepsilon, E/N)$, using

$$F\left(\varepsilon, \frac{E}{N}\right)d\varepsilon = m_e f\left(v_e, \frac{E}{N}\right)v_e dv_e \quad (12)$$

The E/N-dependent electron-impact ionization and attachment coefficients are then given respectively by [62, 63]

$$\frac{\alpha}{N} = \frac{1}{\bar{v}_e}\left(\frac{2}{m_e}\right)^{1/2}\int_0^\infty Q_i(\varepsilon)F\left(\varepsilon, \frac{E}{N}\right)d\varepsilon \quad (13)$$

and

$$\frac{\eta}{N} = \frac{1}{\bar{v}_e}\left(\frac{2}{m_e}\right)^{1/2}\int_0^\infty Q_a(\varepsilon)F\left(\varepsilon, \frac{E}{N}\right)d\varepsilon \quad (14)$$

where $Q_i(\varepsilon)$ and $Q_a(\varepsilon)$ denote the total ionization and attachment cross sections. The drift velocity can also be computed from the kinetic-energy distribution function using the integral expression

$$\bar{v}_e = \frac{-e}{3}\left(\frac{2}{m_e}\right)^{1/2}\frac{E}{N}\int_0^\infty Q_M^{-1}\frac{dF}{d\varepsilon}d\varepsilon \quad (15)$$

where Q_M is the momentum transfer cross section.

Equations (13) and (14) imply an average over a large number of electrons. It can thus be argued [35] that the ionization and attachment coefficients as defined by these equations have no meaning in the early stages of discharge growth when there are only a small number of electrons in the discharge gap. Moreover, the steady-state condition implied by Equation (11) breaks down if there is a sufficiently rapid change in the electric field with time or with position. The meaning of the coefficients is therefore also questionable in the immediate vicinity of a sharp electrode where there can be a large gradient in the electric field. It is necessary to keep these limitations in mind when ionization and attachment coefficients are used to model discharges [64].

It should be realized that the forms of Equation (1) to (3) imply simplifications and assumptions that are not always clearly stated. For example, it is tacitly assumed in writing Equation (3) that only one type of negative ion is formed in the discharge. As is shown in Table 2 for the case of pure oxygen, there is the possibility of forming more than one type of negative ion. Moreover, there are reactions that convert one negative ion into another, and

Table 2.
Examples of reactions involving formation, destruction, and conversion of negative ions in oxygen.

$e + O_2 + M$	$\rightarrow$	$O_2^- + M$
		$[M = O_2, O, O_3, O_2(^1\Delta_g)]$
$e + O_2$	$\rightarrow$	$O_2^- + hv$
$e + O_2$	$\rightarrow$	$O^- + O^+ + e$
$e + O_2$	$\rightarrow$	$O^- + O$
$e + O_2\ (^1\Delta_g) + M$	$\rightarrow$	$O_2^- + M$
		$[M = O_2, O, O_2\ (^1\Delta_g)]$
$O^- + O$	$\rightarrow$	$O_2 + e$
$O^- + O_2^+$	$\rightarrow$	$O + O_2$
$O^- + O_2\ (^1\Delta_g)$	$\rightarrow$	$O_3 + e$
$e + O^-$	$\rightarrow$	$O + 2\,e$
$O^- + M$	$\rightarrow$	$O + M + e$
		$[M = O_2]$
$O_2^- + O_2\ (^1\Sigma_g^+)$	$\rightarrow$	$2\,O_2 + e$
$O^- + O_3$	$\rightarrow$	$O_3^- + O$
$O_2^- + O_3$	$\rightarrow$	$O_3^- + O_2$
$O_2^- + O$	$\rightarrow$	$O^- + O_2$

destruction of negative ions can occur by processes other than ion-ion recombination. To be more complete, Equation (3) could be replaced with a set of coupled equations for the different negative ions represented by

$$\frac{\partial N_{ni}}{\partial t} = N_e \eta_i |\vec{v}_e| - N_{ni} N_p \beta_{2i} - \nabla \cdot (\vec{v}_{ni} N_{ni}) + \nabla^2 (D_{ni} N_{ni}) + \left[\sum_j k_{jk} N_{nj} N_k - \sum_k k_{ki} N_{ni} N_k - N_e k_{ei} N_{ni} \right] \quad (16)$$

where $N_{ni} (i = 1, 2, \cdots)$ is the number density of the ith negative-ion species and the added term in brackets is a source-sink term that allows for ion conversion and negative-ion destruction by collisional detachment. Here k_{jk} of the first term in brackets is the reaction rate coefficient for conversion of the jth ion species into the ith species by reaction with a molecular species of density N_k. Similarly, the second term corresponds to conversion of the ith species into another species and the last term corresponds to collisional detachment by electron impact. In some cases, it may also be necessary to include additional negative-ion processes such as photodetachment and detachment by heavy particle collisions [65, 66].

When the multitude of different reactions is considered, it can be seen that the formulation of the problem takes on a significant added complexity. Generally it can be expected that most of the many possible processes are relatively unimportant and can usually be safely neglected. Ideally one should start with as complete a model as possible and eliminate processes only after performing a sensitivity analysis that determines their relative importance [48].

Simplified models such as based on Equations (1) to (4) are usually deterministic in the sense that they always yield the same result for a given set of boundary conditions, *e.g.*, the predicted PD current pulse amplitude and shape can have no statistical variability. In reality, PD current pulses exhibit significant statistical variation. The statistical distributions of PD pulse parameters such as amplitude, shape, and time-of-occurrence can be derived when the statistical natures of the initiatory electron release and initial electron avalanche growth are considered [13, 28]. Statistical variations in PD behavior are often largely determined by the effects of pulse-to-pulse memory propagation whereby residual space charge, *etc.* left behind by a PD pulse will influence the probabilities for initiation and development of subsequent pulses. The importance of memory effects in determining the statistical properties of pulsating PD is shown in Section 4.

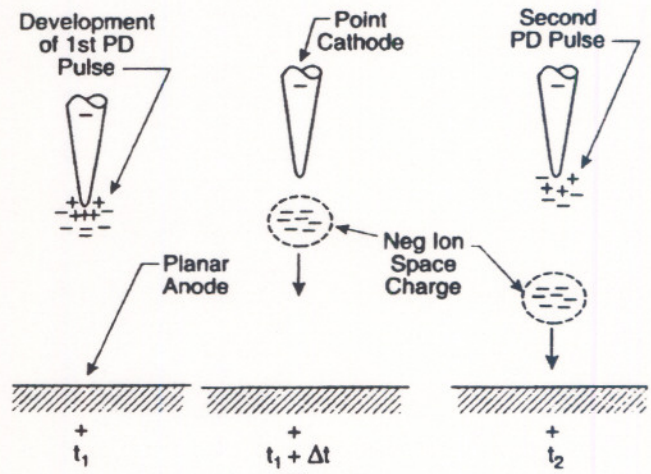

Figure 3.
Motion of ion space associated with pulsating negative corona generated by a point-plane electrode configuration in an electronegative gas. Indicated are successive times, $t_1, t_1 + \Delta t$, and t_2 after extinction of the first corona pulse up to the initiation of the second pulse ($\Delta t < t_2 - t_1$).

4. STOCHASTIC BEHAVIOR AND MEMORY EFFECTS

4.1. dc DISCHARGES

It is known that pulsating PD phenomena can exhibit complex stochastic behavior in which 'memory effects' play an important role [28]. The importance of

memory effects was first established from the measurement of various conditional and unconditional PD pulse-amplitude and time-separation distributions for negative point-plane Trichel-pulse corona [9, 67, 68]. In the case of Trichel pulses, the memory effect results from the influence of space charge and metastable excited species generated during a discharge pulse on the initiation and growth of subsequent discharge events as illustrated by the diagram shown in Figure 3 that was suggested in the work of Lama and Gallo [69].

The pulsating nature of negative corona that occurs in electronegative gases like O_2 and SF_6 is a consequence of the accumulation of a negative-ion space charge in the gap that causes a reduction of the electric-field strength below the level needed to sustain the discharge. The next discharge pulse occurs only after the ion space charge has moved sufficiently far away from the point electrode to allow restoration of the field to the level required for discharge initiation and growth. However, the presence of negative-ion space charge 'clouds' in the gap from previous events will tend to reduce the field strength near the point and thus affect the environment in which the next pulse develops. The discharge model discussed in Section xx which was used by Morrow [12, 49] to describe Trichel pulses in oxygen only applies to the first pulse because it does not consider the modifications of gap conditions due to previous pulses.

Because the initial growth of a discharge pulse depends exponentially on the local field strength, it can be expected that the 'size' of a discharge pulse, as measured for example by its amplitude or integrated charge, will be sensitive to the small reductions in the field at the point electrode due to the presence of space-charge clouds in the gap. The significant effect of space-charge clouds on the growth of Trichel pulses was demonstrated [67] from measurement of conditional pulse amplitude distributions $p_1(q_n|\Delta t_{n-1})$, which give the probability that the nth discharge pulse will have an amplitude between q_n and $q_n + dq_n$ if its time separation Δt_{n-1} from the previous event is restricted to lie within a narrow window between Δt_{n-1} and $\Delta t_{n-1} + \delta(\Delta t_{n-1})$.

Figure 4 shows examples of normalized conditional negative-corona pulse amplitude distributions measured by Kulkarni and Van Brunt [70] for different indicated values for Δt_{n-1}. These results were obtained for a point-plane gap in an SF_6/O_2 mixture containing 10% SF_6 for an absolute pressure of 100 kPa, a point-plane gap of 1.7 cm, and a gap voltage of 14.0 kV. The expectation values defined by

$$\langle q_n(\Delta t_{n-1})\rangle = \int_0^\infty q_n p_1(q_n|\Delta t_{n-1}) dq_n \qquad (17)$$

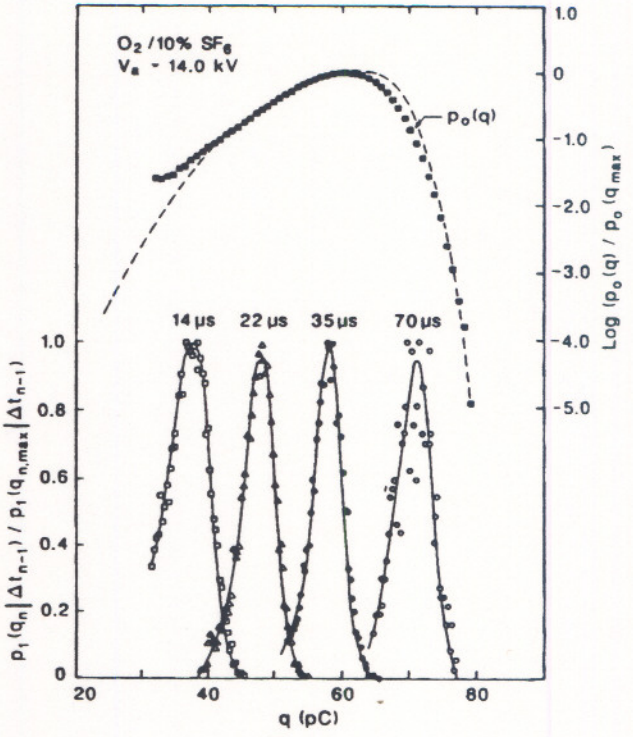

Figure 4.

Normalized conditional pulse-amplitude distributions for negative point-plane corona pulses in a O_2/10% SF_6 mixture for the indicated fixed time separations Δt_{n-1}, compared with the corresponding measured and calculated normalized unconditional pulse-amplitude distributions [61]. The calculated distribution (dashed line) was obtained from the measured $p_1(q_n|\Delta t_{n-1})$ and $p_o(\Delta t_{n-1})$ using Equation (18). The solid lines are Gaussian fits to the $p_1(q_n|\Delta t_{n-1})$ distributions.

show a pronounced dependence on Δt_{n-1}, namely $\langle q_n(\Delta t_{n-1})\rangle$ increases with increasing Δt_{n-1}. This is an expected trend since the greater the time separation from the previous discharge event the greater will be the distance that the negative ion space-charge clouds will have moved away from the point electrode, and consequently the greater will be the local field in which the next discharge event develops.

The conditional amplitude distributions are compared in Figure 4 with the corresponding unconditional amplitude distribution $p_o(q_n)$, measured under the same condition. The fact that $p_o(q_n) \neq p_1(q_n|\Delta t_{n-1})$ for an arbitrary Δt_{n-1} implies that there exists a correlation between the random variables q_n and Δt_{n-1}. Because of the dependence of q_n on Δt_{n-1}, the distribution $p_o(q_n)$ is related to the time separation distribution function,

$p_o(\Delta t_{n-1})$, by the integral

$$p_o(q_n) = \int_{\Delta t_c}^{\infty} p_o(\Delta t_{n-1}) p_1(q_n|\Delta t_{n-1}) d(\Delta t_{n-1}) \quad (18)$$

where Δt_c is the minimum pulse-to-pulse time separation required for restoration of the local field to a value that is high enough to allow the growth of a discharge pulse. The result of performing this integration using the corresponding measured time-separation distribution is shown by the dashed line in Figure 4 which is in reasonable agreement with the measured $p_o(q_n)$ distribution. From this analysis, it is clear that the statistical spread in corona pulse amplitudes is determined largely by pulse-to-pulse memory propagation.

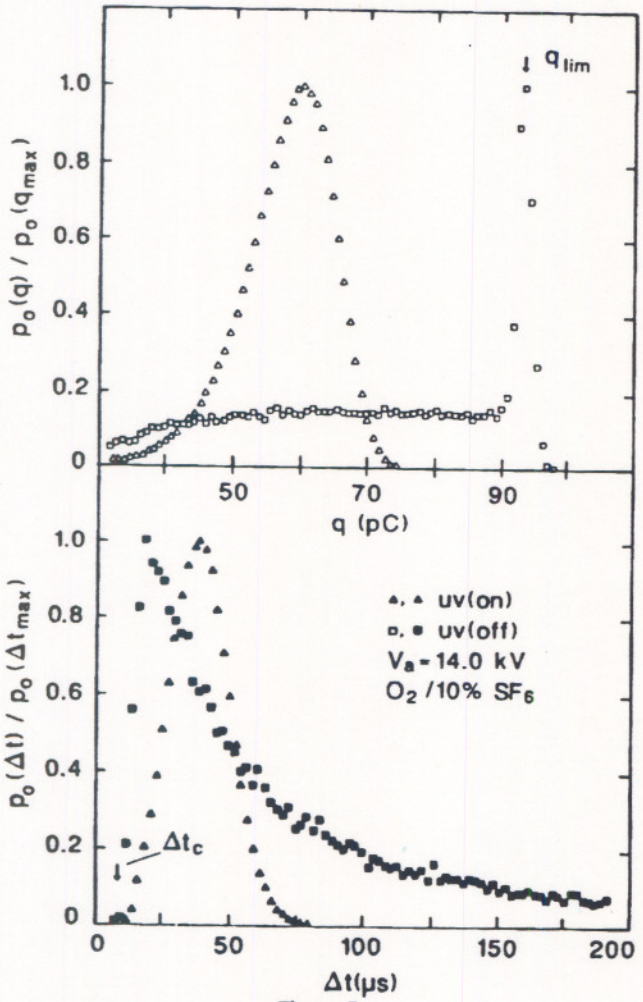

Figure 5.

Normalized pulse amplitude and corresponding pulse time separation distributions for negative point-plane corona pulses in a O_2/10% SF_6 mixture obtained with and without ultra-violet irradiation of the point [61].

It can be inferred from Equation (18) that any changes which occur in the time separation distribution of the corona pulses will necessarily produce changes in the corresponding pulse-amplitude distributions. This is illustrated in Figure 5 which shows corresponding unconditional amplitude and time separation distributions measured for point-plane negative corona pulses in a O_2/10% SF_6 gas mixture with and without exposure of the point to ultra-violet radiation [60]. When radiation is present, it artificially enhances the rate for release of initiatory photoelectrons from the point and thus reduces the mean time between pulses. It is seen that when the radiation is on, the distribution $p_o(\Delta t_n)$ is narrower and shifted to lower Δt_n values than when the radiation is absent. The corresponding $p_o(q_n)$ also becomes narrower and yields a lower mean value for q_n when the radiation is on. In the absence of radiation, $p_o(q_n)$ exhibits a sharp peak at a value denoted in Figure 5 as q_{lim}. This is the limiting maximum mean value of the amplitude for corona pulses that occur in a gap free of space charge and corresponds to time separations from the previous pulse that are greater than about 80 μs which is the approximate minimum time required for a negative-ion cloud to make a transit across the gap.

The gap transit time Δt_l for negative ions can be estimated using the expression

$$\Delta t_l \simeq \frac{1}{\mu} \int_0^{Z_d} dZ [E(Z)]^{-1} \quad (19)$$

where Z_d is the point-to-plane gap distance, E is the unperturbed axial electric-field strength, and μ is the ion mobility which is assumed to be independent of E. Thus, there should be a loss of memory due to space charge from previous corona pulses if $\Delta t_{n-1} > \Delta t_l$. Successive pulses that satisfy this condition are essentially equivalent to the 'first' pulses treated in Morrow's model.

A more complete stochastic analysis of Trichel pulses [67] has shown that both the amplitude of a pulse and its time separation from a previous pulse are, in general, correlated with the amplitudes and time separations of all previous pulses, *i.e.*, the Trichel-pulse phenomenon is a non-Markovian process in which memory can extend indefinitely back in time. Moreover, the complete analysis reveals that there are other sources of memory propagation such as that associated with metastable excited species produced during previous PD events which affect not only the growth of subsequent events through a local enhancement of the ionization coefficient, but also the discharge initiation probability through electron ejection by metastable quenching on the surface of the point electrode. The ion space charge dominated memory effect evident from the conditional pulse-amplitude

distributions shown here for SF_6/O_2 gas mixtures is consistent with results obtained for other electronegative gas mixtures such as N_2/O_2 and Ne/O_2 [67, 71].

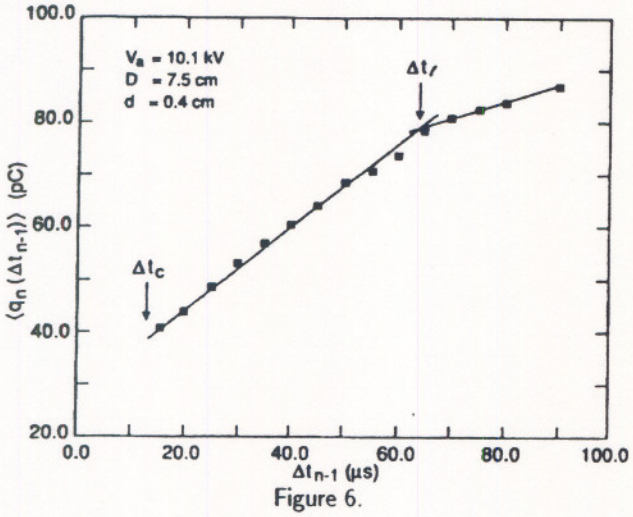

Figure 6.

The expectation value $\langle q_n(\Delta t_{n-1})\rangle$ *vs.* Δt_{n-1} for dc negative PD pulses generated at a point electrode separated in air from a 7.5 cm diameter PTFE surface by a distance of 0.4 cm [63].

When a solid dielectric such as polytetrafluoroethylene (PTFE) is placed on the surface of the plane electrode in a point-plane gap, it is found [72] that Trichel pulses still occur when the point is negative, even at relatively small gap spacings. Moreover, for most point-dielectric spacings at which Trichel pulses occur, the dominant memory effect is still that due to the motion of negative-ion space charge. At sufficiently small spacings, there is evidence of a memory effect due to the accumulation and decay of charge on the dielectric surface. This is illustrated by the data in Figure 6 which which shows a plot of $\langle q_n(\Delta t_{n-1})\rangle$ *vs.* Δt_{n-1} for negative corona pulses generated using a point electrode located 0.4 cm from a PTFE surface in air. Also marked on this Figure are the critical minimum time between successive pulses Δt_c, and the gap transit time Δt_l, estimated using Equation (19). It is seen that even for $\Delta t_{n-1} > \Delta t_l$ there is an increase of $\langle q_n(\Delta t_{n-1})\rangle$ with Δt_{n-1}, albeit a slower increase than for $\Delta t_{n-1} < \Delta t_l$. It is speculated that for $\Delta t_{n-1} > \Delta t_l$, the memory effect is due predominantly to changes in the electric field at the point that result from a relatively slow dissipation or redistribution of charge deposited on the PTFE surface by previous discharge events. At a small enough gap distance, it is found [72] that the discharge will cease entirely after the occurrence of a relatively small number of pulses. The cessation of the discharge can be attributed to the accumulation of enough quasi-permanent dielectric surface charge beneath the point electrode to keep the local field below the level required for discharge development. The initiation of subsequent discharge activity will depend on the rate of surface-charge dissipation. Under dc conditions, it can therefore be expected that the mean time between PD events which occur within a dielectric cavity can be quite long, *i.e.*, > 5 h.

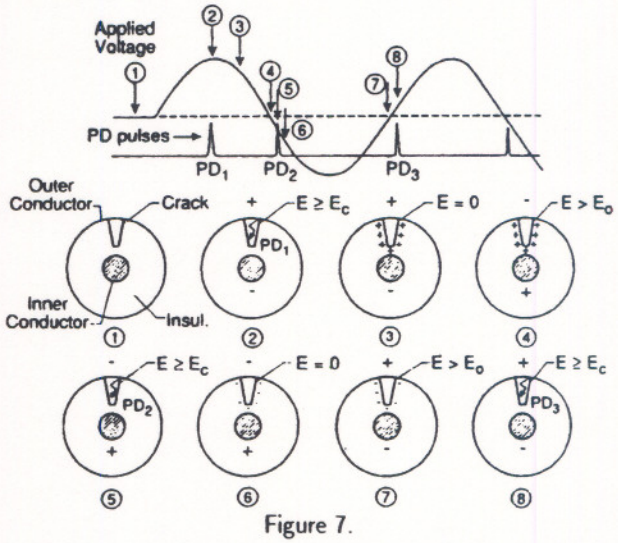

Figure 7.

Illustration of a sequence of PD pulses generated at a 'crack' in the insulation of shielded cable when an alternating voltage is applied.

4.2. ac DISCHARGES

The cessation of PD due to the accumulation of permanent or quasi-permanent charge on dielectric surfaces which happens for constant applied gap voltage need not occur for alternating voltages. This is because the surface charge deposited during any half cycle of the applied voltage will enhance the local field during the subsequent half cycle when the polarity reverses. An example of the situation that can be encountered for alternating voltages is illustrated in Figure 7. For the case shown in this Figure, PD are assumed to occur at a crack in the insulation of a shielded cable. The first PD might occur near the peak of the applied voltage on either half cycle once the local field strength exceeds the inception level denoted by E_c. The charge deposited on the insulator surface by this event will influence the phase-of-occurrence of the next event which is shown to appear near the zero crossing. Because of the deposited charge, the local field strength in the crack will exceed the field E_o that would occur in the absence of this charge as the polarity of the applied voltage changes sign. This explains why the first PD on the next half cycle can occur at or near the zero crossing.

This picture suggests that the predominant memory effect for ac-generated PD which occur on or near insulating surfaces is that due to surface charging. The significant influence of surface charging on phase-to-phase

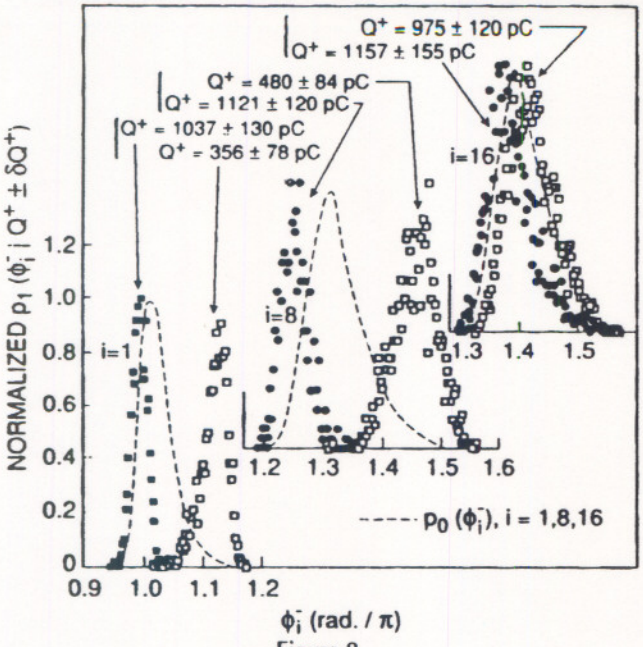

Figure 8.

Normalized conditional and corresponding unconditional phase-of-occurrence distributions of the first, eighth, and sixteenth PD pulses to appear in the negative half cycle for a 1.5 mm point-to-dielectric discharge gap in air at 3.0 kV rms and 200 Hz. The dashed lines correspond to the unconditional distributions and the open and closed points correspond respectively to phase distributions conditioned on the indicated restricted ranges for Q^+ of the previous half cycle [14].

memory propagation for ac-generated PD was first experimentally demonstrated [73] by measuring various conditional probability distributions such as $p_1(\phi_i^-|Q^+)$, where ϕ_i^- is the phase-of-occurrence of the ith negative PD pulse on an arbitrary negative half cycle of the applied voltage and Q^+ is the net integrated charge associated with positive PD on the previous positive half cycle, *i.e.*,

$$Q^+ = \sum_j q_j^+ \tag{20}$$

Examples of measured conditional and unconditional phase-of-occurrence distributions of negative PD pulses previously reported [14] for a point electrode slightly displaced from a PTFE surface are displayed in Figure 8. Given in this Figure are results for the first, eighth, and sixteenth pulses on the negative half cycle. The fact that the mean phase of the first pulse occurs near the zero crossing, *i.e.* $\langle\phi_1^-\rangle \simeq \pi$, suggests the significance of surface charge in enhancing the local field. Moreover, the fact that the unconditional and conditional distributions are not equal even for the sixteenth pulse, *i.e.* $p_o(\phi_{16}^-) \neq p_1(\phi_{16}^-|Q^+)$, implies a correlation between the variables ϕ_i^- and Q^+. The results clearly demonstrate, as expected, that the larger the amount of charge Q^+, the sooner in phase will be the occurrence of negative pulses on the subsequent negative half cycle, *i.e.* as Q^+ increases, $\langle\phi_i^-(Q^+)\rangle$ will decrease, where

$$\langle\phi_i^-(Q^+)\rangle = \int_0^{2\pi} \phi_i^- p_1(\phi_i^-|Q^+)d\phi_i^- \tag{21}$$

The unconditional phase-of-occurrence distributions can be constructed from the conditional distributions using the integral expression

$$p_o(\phi_i^-) = \int_0^{\infty} p_o(Q^+)p_1(\phi_i^-|Q^+)dQ^+ \tag{22}$$

where $p_o(Q^+)$ is the unconditional distribution of integrated positive PD charge in a half cycle.

It is important to point out that the phase-resolved PD pulse-height distributions previously reported by others [7–9, 74], do not contain information about memory propagation. Although phase-resolved distributions are 'conditional' in the sense that they restrict the phase interval of observation, they are not conditional in the sense of either selecting individual pulses according to their order of occurrence or in imposing restrictions related to the behavior of PD that occurred at earlier times (or phases). A physical interpretation of phase-resolved PD data requires an unraveling of memory effects as discussed in the recent work of Van Brunt and coworkers [14]. The complexity of the unraveling process makes it extremely difficult to interpret phase-resolved pulse-height distributions in terms of discharge mechanisms. It can thus be argued that the measurement of selective PD amplitude or phase distributions that are conditioned on a particular past history of the discharge process can provide greater physical insight than the usual phase-resolved distributions.

The PD memory effects considered in this Section are those associated with residuals produced by previous discharge events such as space charge that can dissipate with time. It is this kind of memory effect that largely controls the stochastic behavior of PD at any given time. This effect is also distinct from 'memory effects' associated with aging processes that produce permanent changes of materials or geometrical configuration from which the discharge gap cannot recover. The aging produced by PD contributes to the nonstationary behavior in the stochastic properties of PD that is discussed in Section 5.

5. NONSTATIONARY BEHAVIOR

Nonstationary behavior of PD has been observed under a variety of experimental conditions [18, 19, 26, 27, 75]. By the term nonstationary behavior it is meant that the statistical characteristics of PD such as the pulse height or phase distributions have a dependence on time. It has previously been argued [14] that, because the statistical characteristics of PD are determined largely by memory effects, it can be expected that these characteristics will be susceptible to nonstationary behavior. The susceptibility to nonstationary behavior can be understood from a consideration of the implications of memory effects. If it is found, as shown in Section 4, that the amplitude of a PD pulse depends strongly on its time separation from the previous pulse, then anything that changes the pulse time separation distribution will necessarily, according to Equation (18), also change the amplitude distribution. It will be shown below that the time (or phase) distribution of PD is primarily controlled by the rate of initiatory electron release into the gap, which is, in turn, affected by the local field strength at or near the emitting electrode (or dielectric) surface.

To show the connection between the PD pulse time-separation distribution, $p_o(\Delta t_{n-1})$, and the rate $R_e^{\pm}$ of the electron release from a surface, it will be assumed that the probability for occurrence of a PD between times t and $t + dt$ is proportional to $R_e^{\pm}$ and given by

$$p'_{\pm}(t)dt = R_e^{\pm}(t)\left[1 - \int_0^t p'_{\pm}(t')dt'\right]dt \qquad (23)$$

where the $\pm$ designation refers to the polarity of the applied voltage at the most highly stressed electrode, *e.g.*, the point electrode. The time differential probability function satisfies the requirement

$$\int_0^{\infty} p'_{\pm}(t')dt' \leqslant 1 \qquad (24)$$

The term in brackets on the right-hand side of Equation (23)is the probability that a PD has not occurred up to time t.

In general, $R_e^{\pm}(t)$ depends on time, where, as shown below, the time dependence in a short time frame is most likely governed by the time dependence of the local field, and in a long time frame by aging processes such as result from discharge-induced modification of surfaces that produce changes in the effective work functions. Assuming that t is restricted to a small increment of time δt in which $R_e^{\pm}$ is assumed to be constant, it can be shown that the function which satisfies Equation (23) and (24) has the form

$$p'_{\pm}(t) = R_e^{\pm}\exp(-R_e^{\pm}t) \qquad (25)$$

where $t \in \delta t$. The probability that a PD occurs in the time interval δt is then given by

$$p_{\pm}(\delta t) = \int_0^{\delta t} p'_{\pm}(t')dt' \qquad (26)$$

which gives

$$p_{\pm}(\delta t) = 1 - \exp(-R_e^{\pm}\delta t) \qquad (27)$$

Using a field emission model for electron release from surfaces [13] gives a time dependence for $R_e^{\pm}(t)$ of the form

$$R_e^{\pm}(t) = C_1^{\pm}|E(t)|^2\exp(-C_2^{\pm}/|E(t)|) \qquad (28)$$

where $C_1^{\pm}$ and $C_2^{\pm}$ are factors that are related to the anode, cathode work functions w_+ and w_- by

$$C_1^{\pm} = b_1^{\pm}10^{(b_2^{\pm}w_{\pm}^{1/2})} \qquad (29)$$

and

$$C_2^{\pm} = b_3^{\pm}w_{\pm}^{3/2} \qquad (30)$$

Here b_1, b_2, and b_3 are positive constants.

For the case of a sinusoidal applied voltage of frequency ω, the local field is given by

$$E(t + \delta t) = E_0\sin[\omega(t + \delta t)] - \Delta E_s(t + \delta t) \qquad (31)$$

where the second term on the right-hand side is the contribution to the local field by space charge or surface charge. For a point electrode on or close to the surface of an insulator, the changes in ΔE_s associated with the deposition of surface charge for a PD event are considered to be abrupt provided δt is comparable to or smaller than the intrinsic width of the PD pulse. This means that ΔE_s behaves like a step function where

$$\Delta E_s(t + \delta t) = \Delta E_s(t) \qquad (32)$$

if no PD occurs within δt, and

$$\Delta E_s(t + \delta t) = \Delta E_s(t) \mp \Delta E_j^{\pm} \qquad (33)$$

if the jth positive or negative PD occurs within δt. Here $\Delta E_j^{\pm}$ is the change in local field due to charge deposited on the surface by the jth PD pulse. The behavior of the local field represented by Equation (31) to (33) will, when substituted into Equation (28), give the time dependence for $R_e^{\pm}(t)$.

The PD time-separation distribution can be computed numerically by discretizing each pulse time separation into multiples of δt, *i.e.*,

$$\Delta t_{n-1} = t_n - t_{n-1} = m\delta t \qquad (34)$$

where m is an integer and $\Delta t_{n-1} \gg \delta t$. The probability that the nth pulse will be separated from the $(n-1)$th pulse by a time Δt_{n-1} is then given by

$$p_o(\Delta t_{n-1})d(\Delta t_{n-1}) = \prod_{k=1}^{m-1} \left\{\exp\left[-R_e^{\pm}(k\delta t)\delta t\right]\right\}\left\{1-\exp\left[-R_e^{\pm}(m\delta t)\delta t\right]\right\} \quad (35)$$

which is obtained using Equation (27) and the law of probabilities. Of particular relevance in the present discussion is the strong dependence of $R_e^{\pm}$ on $E(t)$ and also on the surface work functions implied by Equations (28) to (30). The dependence of $R_e^{\pm}$ on $E(t)$ when w_+ and w_- are constant produces the type of 'stationary' memory effect discussed in Section 4, *i.e.*, the statistical distributions represented by $p_o(q_n)$ and $p_o(\Delta t_{n-1})$ do not vary with time. However, time variations in either w_+ or w_- can introduce nonstationary behavior that is reflected in a time dependence of the distributions $p_o(q_n)$ and $p_o(\Delta t_{n-1})$. The numerical procedure discussed above has been used in the formulation of a Monte-Carlo simulator of PD [10, 13, 14, 18] from which various conditional and unconditional PD amplitude, phase, or time distributions can be extracted.

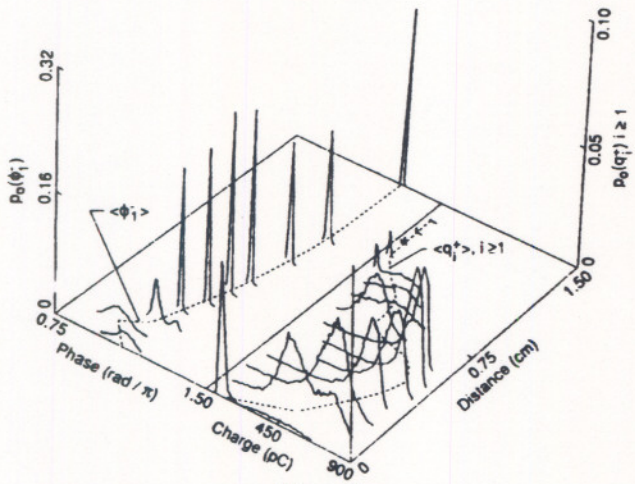

Figure 9.

Measured phase-of-occurrence distributions of the first negative PD pulse and unconditional amplitude distributions of the corresponding positive PD pulses *vs.* distance of a point electrode from a flat PTFE surface in air. Also indicated by the dashed lines are the corresponding mean values $\langle\phi_1^-\rangle$ and $\langle q_i^+\rangle$, $i \geq 1$ [67].

Results of recent experimental investigations indicate that there can be several sources of nonstationary behavior in the statistical characteristics of PD. For example, there is evidence that small changes in the geometrical configuration of a point-dielectric gap such as could result from mechanical motion or removal of material during the discharge, as discussed in Section 6, will produce large changes in the behavior of PD [76]. The sensitivity to gap spacing for PD generated by applying an alternating voltage to a point electrode over a PTFE surface in air is illustrated by the experimental results displayed in Figure 9. This Figure shows measured phase-of-occurrence distributions of the first negative PD pulse and unconditional amplitude distributions of the corresponding positive PD pulses *vs.* point-to-dielectric gap spacing. Also indicated by the dashed lines are the corresponding mean values $\langle\phi_i^-\rangle$ and $\langle q_i^+\rangle, i \geq 1$. The most dramatic change occurs as the gap spacing is increased from 0 to 0.75 cm. The statistical characteristics of PD for the case where the point touches the dielectric are distinctly different from the case where there is a small spacing of 0.5 mm. As the gap spacing increases, the characteristics change from those of a surface discharge to those of a corona discharge, *i.e.*, the presence of the dielectric surface becomes increasingly less important. For gap spacings greater than about 1.20 cm, the positive discharge ceases entirely, and the negative discharge takes on the appearance of a phase-restricted train of Trichel pulses.

Another source of nonstationary PD behavior is that associated with discharge-induced changes in dielectric surface conductivity. It was argued in an earlier work by Rogers [77] that the 'self-extinction' of pulsating PD in a dielectric cavity can be attributed to an increase in the conductivity of the cavity walls that occurs when the discharge is active. More recently, Hudon and coworkers [19] have reported the transformation of a pulsating discharge into a pulseless glow discharge in a gap formed by parallel epoxy resin planes. They showed that this transformation is related to an increase in the surface conductivity of the epoxy. Possible mechanisms for the increase in surface conductivity will be mentioned in Section 6.

Additional evidence of the effect of changing surface conductivity is provided from recent work on point-epoxy gaps [18, 27, 78]. Figure 10 shows examples of integrated charge distributions $p_o(Q^+)$ and $p_o(Q^-)$, measured at different indicated times for discharge pulses generated by applying a 50 Hz, 3.0 kV rms alternating voltage to a sharp point electrode that touches a flat cast epoxy surface. In this case, the epoxy contained Al_2O_3 filler. Also shown in this Figure are the measured mean numbers of positive and negative PD pulses ($\langle n^+\rangle$ and $\langle n^-\rangle$). The significant feature of these results is the disappearance of positive PD pulses after $\sim$ 1.5 h. In the early stages of discharge activity, there is an approximate charge balance, *i.e.* $\langle Q^+\rangle \simeq -\langle Q^-\rangle$, thus suggesting (from charge

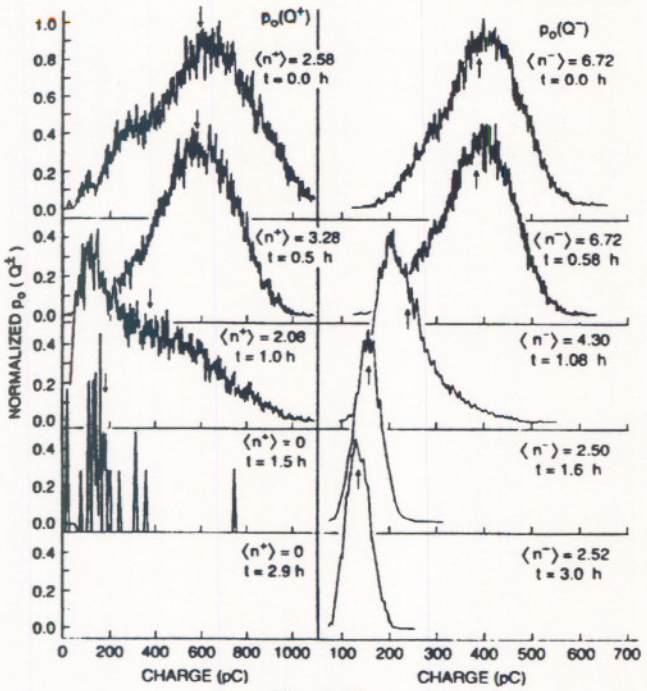

Figure 10.

Positive and negative integrated-charge distributions measured for PD generated by a point electrode touching a flat epoxy surface at the indicated times after a 50 Hz voltage was applied. Also shown are the corresponding mean numbers of positive and negative PD pulses-per-cycle and the mean charge (vertical arrows) [18].

conservation) that all of the discharge current can be accounted for by the observed PD pulses. However, as time progresses, an obvious imbalance occurs which implies that some of the current is not associated with the discharge pulses.

Subsequent measurements (see Section 6) showed that there was a significant increase in epoxy surface conductivity near the discharge site consistent with the observations of Hudon and coworkers [19]. With a modified version of the previously discussed Monte-Carlo simulator, it was possible to show that the disappearance of positive PD is consistent with an increase in the local surface conductivity [18]. Using Poisson's equation coupled with Equation (6) for $s = 0$, and assuming a locally uniform surface conductivity Γ gives the following expression for surface charge density

$$\frac{\partial \sigma}{\partial t} \sim -\Gamma \sigma \tag{36}$$

If it can be assumed that ΔE_s in Equation (31) is proportional to σ at the discharge site, then the solution to Equation (36) leads to an exponential decay in a time interval δt given by

$$\Delta E_s(t + \delta t) = \Delta E_s(t) \exp(-\xi \Gamma \delta t) \tag{37}$$

where $\xi > 0$ is a proportionality constant. In the Monte-Carlo simulation, only the negative surface charge is allowed to decay. The numerical procedure described above is then modified so that if $\Delta E_s(t) \leqslant 0$ and no PD event occurs in the time δt, Equation (32) for $\Delta E_s(t + \delta t)$ is replaced with Equation (37). Equation (32) still applies if $\Delta E_s(t) > 0$ and Equation (33) still applies if a PD event occurs in δt independent of the sign of $\Delta E_s(t)$.

In the original model [13], the effective work function w_+ of the dielectric surface was assumed to be constant, *i.e.*, independent of the local field. To account for the disappearance of positive PD, it was also necessary to assume that the positive PD initiation probability decreases with decreasing negative surface charge density. This was accomplished by giving w_+ a time dependence of the form

$$w_+(t) = a_0 - a_1 \left(\frac{\Delta E_s(t)}{E_o} \right) - a_2 \left(\frac{\Delta E_s(t)}{E_o} \right)^2 \tag{38}$$

for $\Delta E_s(t) < 0$, where a_0, a_1, and a_2 are positive constants. The form implied by Equation (38), although empirical, is considered to be physically reasonable, since the probability for removing an electron from a negatively charged insulating surface should increase with increasing negative-charge density.

Using the model described above, positive PD are found to disappear if [18]

$$\xi \Gamma \geqslant \omega / \pi \tag{39}$$

When this condition is satisfied, the charge deposited by PD during the negative half cycle will have almost completely disappeared when the next positive half cycle begins.

Another contribution to nonstationary behavior that might be especially important under static-gas conditions such as within a cavity of a solid dielectric is that associated with discharge-induced changes in the chemical composition of a gas. An example of nonstationary behavior due to this effect is illustrated by the positive PD pulse-height distributions for SF_6 shown in Figure 11. In this case, the PD were generated using a point-plane gap in an enclosed vessel containing SF_6 at an absolute gas pressure of 200 kPa [79]. In pure SF_6 under these conditions, the point-plane positive corona exhibits a distinctive pulse-burst characteristic [80]. However, after ~ 4 h of operation, the PD burst characteristic is found to be replaced by a continuous chain of pulses that have a relatively lower amplitude, and this is reflected by the change in the pulse-height distribution such as shown

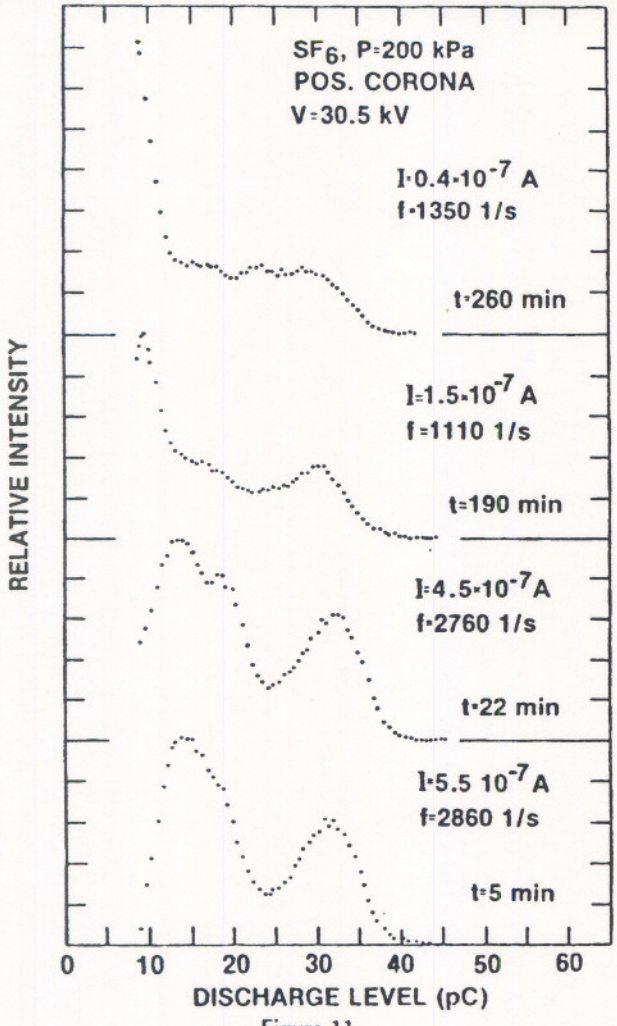

Figure 11.

Time variation of pulse-height distributions for positive-dc-corona pulses in SF_6 at 200 kPa. Also indicated are the corresponding average corona currents I and observed burst pulse repetition rates f [70, 71].

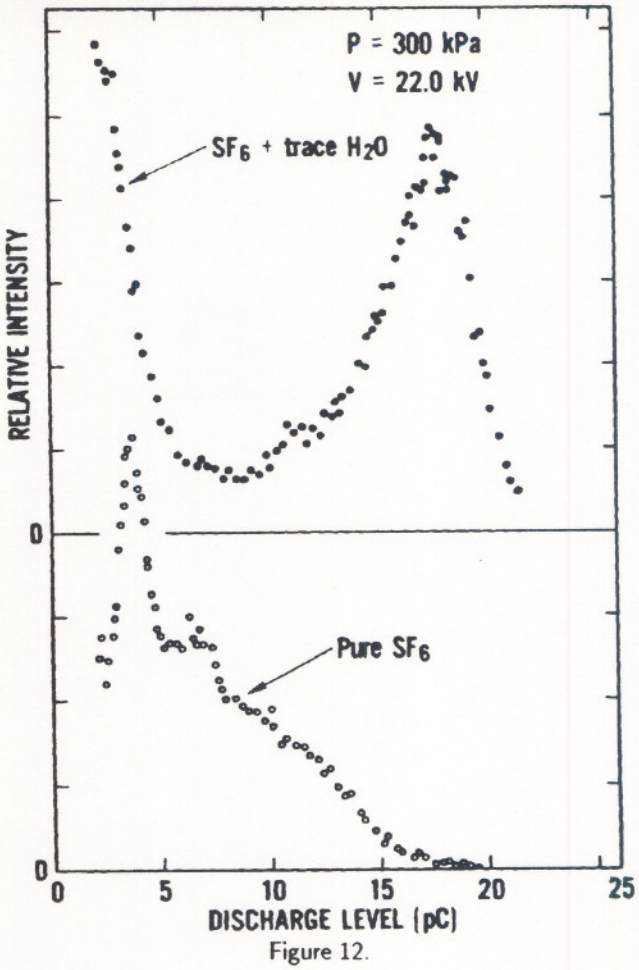

Figure 12.

Measured pulse-height distributions of positive-dc-corona pulses for pure and H_2O-contaminated SF_6 at a gas pressure of 300 kPa [72].

in Figure 12. That the changes seen in Figure 11 were indeed due to changes in the gas composition was verified by replacing the gas in the vessel and restarting the discharge. When this was done, it was found that the amplitude distribution again exhibited a shape similar to that which had appeared initially in the previous test and the same change in PD behavior occurred with increasing time-of-operation.

There is convincing evidence in this case that the observed rapid change in the positive-corona characteristics of SF_6 is due to a buildup of water vapor in the gas during the discharge. Although the source of the water vapor is unknown, it is speculated that it comes from discharge-induced desorption from the electrode surfaces. The change in amplitude distribution seen in Figure 11 can be simulated by adding a trace amount of water vapor to SF_6 as shown in Figure 12 [81].

It is now known that discharge initiation near a positive point electrode can be significantly enhanced by the presence of small quantities of H_2O [82]. The initiation of a corona discharge near a positive point electrode is expected to be due largely to the release of electrons from negative ions by a collisional electron detachment process. It has been shown [83] that in pure SF_6, the only collisional-detachment process which can occur with a reasonable probability is that involving the negative ion F^-, namely

$$F^- + SF_6 \rightarrow F + SF_6 + e \qquad (40)$$

Because of the high threshold energy for this process (8.0 eV), and because F^- is likely to be a minor ion in pure SF_6, the probability of initiation by process (40) is

expected to be quite low for E/N above the critical value needed for ionization growth where $\alpha \geqslant \eta$. On the other hand, when H_2O is added, other types of negative ions such as OH^- can appear [84] that will undergo detachment with orders-of-magnitude higher probability than F^-. It can thus be expected that low levels of water-vapor contamination can have a disproportionately large effect in initiating and maintaining positive corona in SF_6. On a longer time frame, there are other chemical changes in SF_6 discussed in Section xx that could influence the behavior of PD such as through modification of the ionization or attachment coefficients.

The tendency for PD to exhibit nonstationary behavior complicates any attempts to define meaningful statistical patterns that can be used in proposed pattern-recognition schemes based on neural networks, *etc.* for possible identification of the defect sites at which PD occur [85–87]. Nevertheless, the time development of statistical PD patterns may provide additional useful information for identification purposes.

6. PD-INDUCED AGING

When discharges occur in an insulating medium, they can be expected to cause physical and chemical changes of the surrounding material, and in many cases, these changes will be detrimental to the performance of the materials as an electrical insulator. The material changes resulting from exposure to PD are either directly or indirectly a consequence of bombardment of energetic electrons that can have mean energies in excess of 10 eV under breakdown conditions. From a practical point-of-view, the problem of insulation aging has been of paramount concern and there has been extensive research into the mechanisms of aging. In this Section, the focus will be on a few selected aging processes that are relevant to the types of PD phenomena discussed above.

It was pointed out in Section 5 that the exposure of cast epoxy resin surfaces to PD under alternating voltage conditions causes changes in the surface characteristics which can, in turn, influence the behavior of PD. Microscopic examinations of the epoxy surfaces after exposure to PD in air revealed that material had been removed at the discharge site. Results of typical surface profile measurements in the vicinity of a discharge site are shown by the profilograms in Figure 13 [17]. The locations of the point electrode used to generate PD are indicated by the vertical arrows. The epoxy materials used in this case contained an Al_2O_3 filler. The discharges were generated in room air by applying a 4.0 kV rms (50 Hz) voltage to the point electrode for a period of 22 h. In all cases, it was found, as seen in the Figure, that the surface roughness increased significantly at the center of

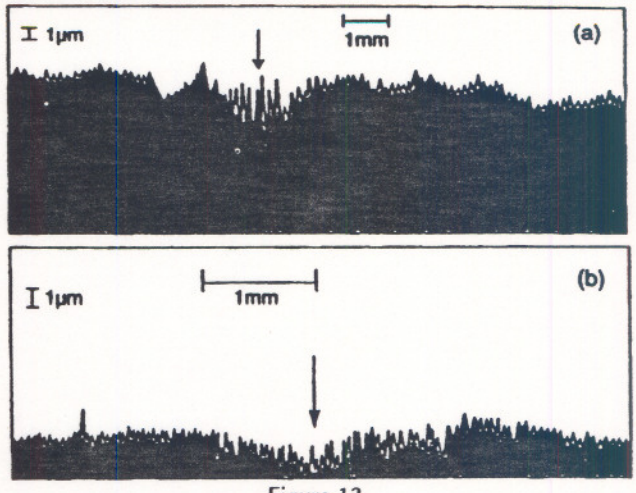

Figure 13.

Profilograms of epoxy surfaces after exposure to PD in air. The vertical arrows indicate the location of the point electrode [17].

discharge activity. The measurements before and after PD exposure showed that there was a volume decrement indicating that material had been removed. For longer PD exposures, narrow channels appeared that are perhaps the precursors to tree formation [26, 75]. Changes in surface profiles such as seen in Figure 13 can also change the local electric-field strength as well as the ability of the surface to trap charged particles. Removal of dielectric material by PD can be safely considered as a 'permanent' alteration or aging effect.

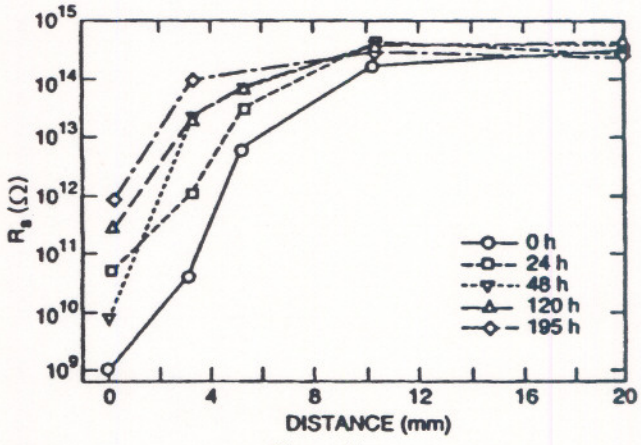

Figure 14.

Measured changes in epoxy surface resistance *vs.* distance from the center of the PD site for different times since the termination of discharge exposure in air [17].

It was noted that PD also cause increases in the local surface conductivity of epoxy. Figure 14 shows the results from measurements of the epoxy surface resistance

vs. distance from the center of the discharge site for different indicated times since the termination of discharge exposure. The discharge conditions were similar to those that produced the surface damage shown in Figure 13. The resistances were measured by moving small parallel wires across the epoxy surface as described previously [17,18]. The change in surface conductivity at the discharge site appears to be 'quasi-permanent' in a sense that the conductivity will, given a sufficiently long time after PD exposure, decrease to a value closer to that observed before initiation of the discharge. This is illustrated by the trend shown in Figure 14. Moreover, wiping the surface with a damp cloth tended to restore the conductivity to the pre-discharge value [17].

The precise nature of the PD-induced physical and chemical changes of epoxy surfaces that give rise to an increase in surface conductivity remain unknown. The fact that the predischarge condition can be largely restored after wiping suggests that the changes are likely due to formation of deposits. There is evidence from the work of Hudon and coworkers [22] that droplets of glycolic and formic acid are formed on epoxy surfaces during exposure to PD. These acids are known to be far more conductive than the epoxy resin matrix.

A necessary condition for the formation of PD is that the mean energy of electrons should be sufficiently high to cause a net growth in the ionization of the gas. Specifically for electronegative gases, this requires that $\alpha > \eta$. Under this condition, the electron energies are also high enough to produce molecular dissociation leading to the formation of highly reactive free radicals such as O, OH, F, and SF_5 by processes like

$$e + O_2 \rightarrow O + O + e \tag{41}$$

and

$$e + SF_6 \rightarrow SF_n + (6 - n)F + e \tag{42}$$

where n is an integer satisfying the restriction $1 \leqslant n \leqslant 5$. These reactive fragments can then lead to the formation of other reactive species. In the case of SF_6/O_2 mixtures, the discharge byproducts are known to include SO_2, SOF_2, SO_2F_2, SOF_4, SF_4, S_2F_{10}, S_2OF_{10}, $S_2O_2F_{10}$, and HF [15,16]. Examples of fast neutral reactions in the active discharge zone that occur in SF_6 corona when O_2 and H_2O are present are listed in Table 3. Species like F and HF will attack solid insulating surfaces and contribute to the removal of material.

As seen from Table 3, the gas-phase chemistry associated with PD phenomena can be very complex. The decomposition of SF_6 in corona discharges has been extensively investigated in recent years because of the widespread use of SF_6 as an insulating medium in HV apparatus and related concerns about toxicity and corrosiveness of the discharge byproducts [15,16,88–90].

Table 3.

Examples of important fast reactions that occur in the discharge zone of a negative corona in SF_6 containing H_2O and O_2. M = third body.

Reaction			Rate coeff. cm^3/s
$F + H_2O$	$\rightarrow$	$OH + HF$	9.0×10^{-12}
$OH + SF_5$	$\rightarrow$	$SOF_4 + HF$	1.1×10^{-12}
$SF_5 + O + M$	$\rightarrow$	$SOF_5 + M$	1.0×10^{-11}
$SOF_5 + SF_5$	$\rightarrow$	$SOF_4 + SF_6$	1.0×10^{-13}
$SF_5 + O$	$\rightarrow$	$SOF_4 + F$	2.0×10^{-11}
$SF_3 + O$	$\rightarrow$	$SOF_2 + F$	1.0×10^{-12}
$SF_5 + F + M$	$\rightarrow$	$SF_6 + M$	1.5×10^{-11}
$SF_3 + F + M$	$\rightarrow$	$SF_4 + M$	2.4×10^{-11}
$SF_5 + SF_5 + M$	$\rightarrow$	$S_2F_{10} + M$	1.4×10^{-12}
$SF_3 + SF_3$	$\rightarrow$	$SF_2 + SF_4$	2.2×10^{-12}
$SF_3 + SF_5$	$\rightarrow$	$SF_6 + SF_2$	5.0×10^{-12}

Figure 15 shows examples of data on the production rates for the major sulfur-containing oxyfluoride by-products from negative point-plane corona discharges in SF_6 [91]. These results were obtained using a continuous constant-current negative-glow corona operated at 40 μA for a total absolute gas pressure of 200 kPa. Shown in Figure 15 are the charge rates of production normalized to the SF_6 concentration as given by

$$r(X) = \frac{1}{I_d[SF_6]}\left(\frac{d[X]}{dt}\right) \tag{43}$$

where I_d is the discharge current, $[X]$ is the quantity in moles of the by-product of interest, and $[SF_6]$ is the absolute quantity of SF_6 in moles. The total oxyfluoride production given by

$$r_t = r(SOF_4) + r(SOF_2) + r(SO_2F_2) \tag{44}$$

is compared in Figure 15 with the estimated maximum possible SF_6 decomposition rate $r_t(\max)$. The estimate of the maximum rate is based on using the calculated rate for reaction (42) [61] in a model of the discharge [47,48], and assuming that every sulfur-containing fragment (SF_n) converts to an observable by-product.

The tendency of r_t to fall considerably below $r_t(\max)$ is a consequence of the fact that recombination reactions such as

$$SF_5 + F + SF_6 \rightarrow 2\,SF_6 \tag{45}$$

are fast at moderately high gas pressures and therefore very efficient in reforming SF_6 after it has been dissociated. The increase in r_t with increasing oxygen content is primarily a consequence of the diluting effect of O_2 which

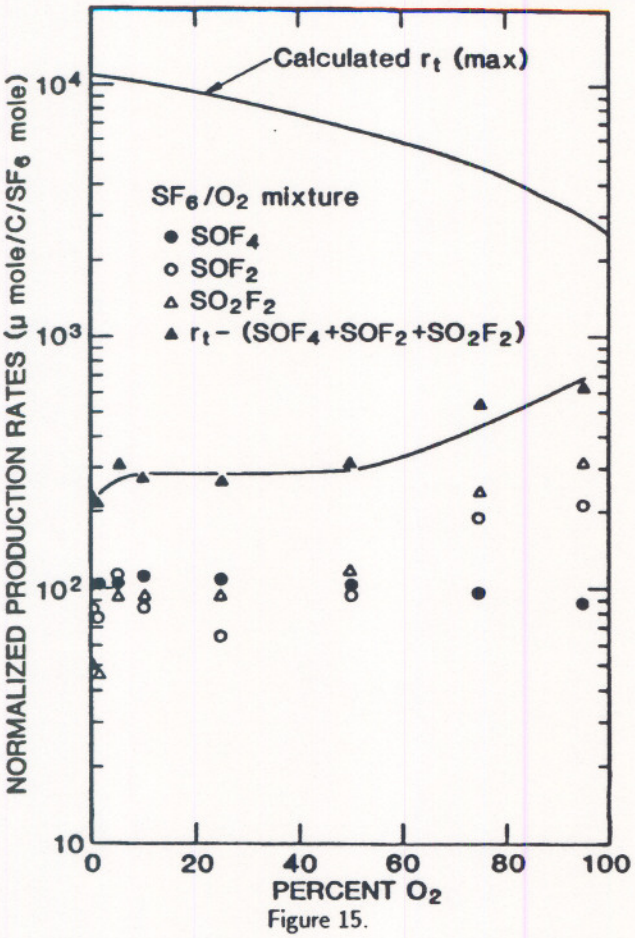

Figure 15.

Measured charge rates-of-production of the oxyfluorides SOF_4, SOF_2, and SO_2F_2 from negative dc point-plane glow-type corona in SF_6/O_2 mixtures [81]. Also shown are the net oxyfluoride production rate r_t, and the calculated maximum SF_6 destruction rate in the discharge r_t(max). The production rates have been normalized to the SF_6 concentration. The discharge current was 40 μA and the total pressure was 200 kPa.

can inhibit the recombination reactions such as process (45).

Under the discharge conditions that yielded the results shown in Figure 15, it was found that other gaseous byproducts can be formed which are not derived from SF_6 dissociation, *i.e.*, they contain neither sulfur nor fluorine. Among these is the gaseous compound CO_2. Shown in Figure 16 are examples of the measured yields of CO_2 *vs.* net charge transported given by the product of discharge current and time. The data in this Figure were obtained for a 40 μA glow-type negative corona in the three indicated SF_6/O_2 mixtures at an absolute total gas pressure of 200 kPa. For these experiments, a stainless steel point electrode was used. It is speculated that the CO_2 is

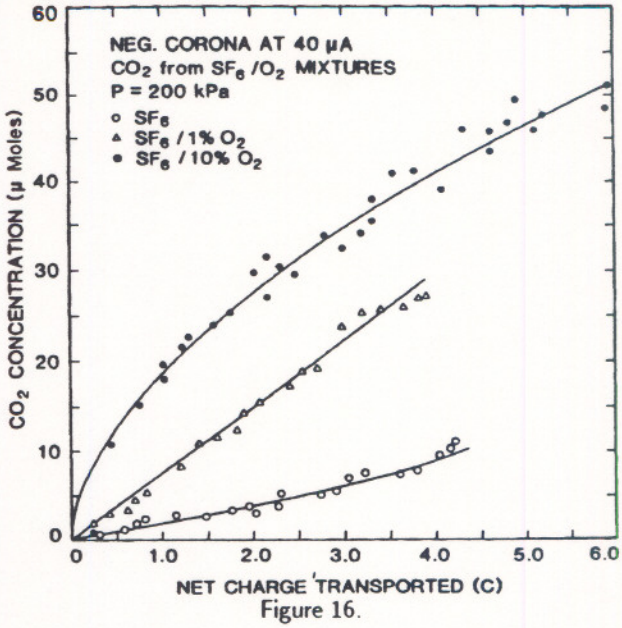

Figure 16.

Measured yields of CO_2 *vs.* net charge transported in a 40 μA negative glow corona in SF_6 and indicated mixtures of SF_6 with O_2.

derived from reactions of oxygen with carbon contained in the steel electrode. The rate for CO_2 production is seen to increase with oxygen content as expected.

The production of CO_2, even in relatively pure SF_6, may be a good indication of so called 'electrode conditioning'. During a negative-corona discharge, the point electrode can be eroded by ion bombardment. This is manifested by the appearance of increased surface roughness or micro-pits at the tip of the electrode. The discharge-enhanced roughness of the electrode surface can cause it to become a more efficient emitter of electrons [80] and can cause an increase in the catalytic destruction of some relatively unstable byproducts such as S_2F_{10} [90].

The production rates for SF_6 byproducts from corona or PD implied by the results shown in Figure 15 suggest that under practical conditions where the volume of SF_6 is relatively large, the buildup of byproducts from the discharge will be too slow to significantly affect the ionization, attachment, and recombination coefficients of the gas. On the other hand, if the decomposition occurs in a small volume such as in a dielectric cavity, it is possible that a large fraction of the gas can become decomposed in a short time, and this could significantly modify the discharge behavior. In general, if the gas consists of more than one component, then the ionization coefficient given by Equation (13) must be replaced by

the sum [63]

$$\frac{\alpha}{N} = \frac{1}{\bar{v}_e}\left(\frac{2}{m_e}\right)^{1/2} \sum_j \frac{N_j}{N} \int_0^\infty Q_{ij}(\epsilon) F(\epsilon, \tfrac{E}{N})\, d\epsilon \quad (46)$$

where Q_{ij} is the ionization cross section of the jth component of density N_j, and

$$N = \sum_j N_j \quad (47)$$

Similar modifications would need to be made in η and other coefficients. Hence, if N_j changes with time due to discharge-induced modifications of the gas, then so will the ionization coefficients, *etc.*, and likewise also the discharge characteristics.

To date, there have not been many attempts to model the chemistry in PD. Only recently has a successful model been formulated for SF_6, and this is restricted to negative-glow type discharges in point-plane gaps [47,48]. Some success has also been achieved in modeling the chemistry of pulsating dielectric barrier discharges in oxygen [39]. The task of modeling the chemistry in PD is quite formidable as can be appreciated when it is realized that Tables 1 and 2 list only a small fraction of the many hundreds of possible chemical processes that may need to be considered.

7. CONCLUSIONS AND RECOMMENDATIONS

EVIDENCE is provided here of significant progress that has been made in achieving a better understanding of the physical and chemical bases of PD phenomena. If anything is to be gained from reading this work, it should hopefully be an appreciation of the fact that PD phenomena are enormously complex. In attempts to explain PD behavior, caution must be exercised in making simplifying assumptions about the relevant mechanisms.

As is often the case with basic research, the increase in knowledge about PD raises more questions and places ever greater demands on the quality of fundamental data needed to carry us up to the next level of understanding. In pursuit of this next level, it is recommended that emphasis be given to the following avenues of research: (1) extend computer simulations of discharge growth to include the modifications of the local environment by residuals from prior discharge activity; (2) develop models that can predict the transition from a pulsating corona to a glow discharge; (3) develop models that predict the size of constricted glows in highly nonuniform fields; (4) perform experiments and calculations to give more information about the influence of high local fields on secondary electron emission from surfaces due to impact of photons, ions, and metastable species; (5) develop better experimental and theoretical techniques to investigate the dynamics of dielectric surface charging during PD activity; (6) acquire more information about changes in PD behavior during electrical tree formation in solids; (7) develop better diagnostics to investigate permanent and quasi-permanent changes in the composition and morphology of solid surfaces exposed to PD; (8) extend measurements of PD-induced decomposition of dielectric gases to lower currents and pulsating PD conditions; (9) develop spectroscopic or other nonintrusive methods for measuring temperature profiles in PD; and last but not least, (10) give special attention to determination of the effects of absorbed and gas-phase H_2O on PD behavior. In reality, there is a much greater number of avenues than suggested here for future basic research on PD that is at least as great as the multitude of different modes of discharge activity. There is yet much more to be learned about PD, and as more is learned, this information can hopefully be put to good use in constructing better diagnostics of insulation performance. I caution against undertaking new large scale efforts to develop practical PD diagnostics without a good understanding of the phenomena being observed.

J. B. Whitehead, for whom this lecture series is named, was fascinated and concerned with corona discharge phenomena in insulation, and conducted significant pioneering research on this topic [92]. It can be argued that the following comments offered in the conclusions of his 1910 paper [92] on the dielectric strength of air are relevant today:

> "Corona formation and the laws which regulate it are of the first importance for electrical engineers since corona is to be prevented both as a source of loss and as an enemy of insulation. The field is replete with fascinating problems. Their solution however involves the use of methods and apparatus generally not familiar to the physicist. "

ACKNOWLEDGMENT

This work was performed in the Electricity Division, Electronics and Electrical Engineering Laboratory, National Institute of Standards and Technology, Technology Administration of the U. S. Department of Commerce. The author is grateful for support provided by the National Institute of Standards and Technology, the U. S. Department of Energy, the U. S. Nuclear Regulatory Commission, and the Electric Power Research Institute, and for major contributions from S. V. Kulkarni, M. C. Siddagangappa, A. V. Phelps, T. Las, E. W. Cernyar, P. von Glahn, H. Slowikowska, J. T. Herron, K. L. Stricklett, J. K. Olthoff, and M. Misakian.

REFERENCES

[1] M. G. Danikas, "The Definitions Used for Partial Discharge Phenomena", IEEE Trans. Elec. Insul., Vol. 28, pp. 1075–1081, 1993.

[2] B. H. Ward, "Digital Techniques for Partial Discharge Measurements-A Report on the Activities of the Working Group on Digital Analysis of Partial Discharges", IEEE Trans. Power Delivery, Vol. 7, pp. 469–479, 1992.

[3] M. Cernak, T. Kaneda and T. Hosokawa, "First Negative Corona Pulses in 70% N_2 + 30% SF_6 Mixture", Japanese J. Appl. Phys., Vol. 28, pp. 1989–1996, 1989.

[4] R. Bartnikas and J. P. Novak, "On the Character of Different Forms of Partial Discharge and their Related Terminologies", IEEE Trans. Elec. Insul., Vol. 28, pp. 956–968, 1993.

[5] T. V. Blalock, A. L. Wintenberg and M. O. Pace, "Low Noise Wide-band Amplification System for Acquiring Prebreakdown Current Pulses in Liquid Dielectrics", IEEE Trans. Elec. Insul., Vol. 24, pp. 641–647, 1989.

[6] F. H. Kreuger, E. Gulski and A. Krivda, "Classification of Partial Discharges", IEEE Trans. Elec. Insul., Vol. 28, pp. 917–931, 1993.

[7] T. Okamoto and T. Tanaka, "Novel Partial Discharge Measurement Computer-aided Measurement Systems", IEEE Trans. Elec. Insul., Vol. 21, pp. 1015–1016, 1986.

[8] B. Fruth and L. Niemeyer, "The Importance of Statistical Characteristics of Partial Discharge Data", IEEE Trans. Elec. Insul., Vol. 27, pp. 60–69, 1992.

[9] R. J. Van Brunt and S. V. Kulkarni, "Method for Measuring the Stochastic Properties of Corona and Partial-discharge Pulses", Rev. Sci. Instrum., Vol. 60, pp. 3012–3023, 1989.

[10] R. J. Van Brunt and E. W. Cernyar, "System for Measuring Conditional Amplitude, Phase, or Time Distributions of Pulsating Phenomena", J. Res. Nat. Inst. Stand. and Tech., Vol. 97, pp. 635–672, 1992.

[11] V. Köpf and K. Feser, "Possibilities to Improve the Sensitivity of PD-Measurements by Using Digital Filters", Proc. Int. Symp. on Digital Techniques in HV Measurements, Toronto, Canada, pp. 2–27–2–31, 1991.

[12] R. Morrow, "Theory of Negative Corona in Oxygen", Phys. Rev. A, Vol. 32, pp. 1799–1809, 1985.

[13] R. J. Van Brunt and E. W. Cernyar, "Stochastic Analysis of ac-generated Partial-discharge Pulses from a Monte-Carlo Simulation", 1992 Annual Report-Conference on Electrical Insulation and Dielectric Phenomena, IEEE, NY, pp. 427–434, 1992.

[14] R. J. Van Brunt, E. W. Cernyar and P. von Glahn, "Importance of Unraveling Memory Propagation Effects in Interpreting Data on Partial Discharge Statistics", IEEE Trans. Elec. Insul., Vol. 28, pp. 905–916, 1993.

[15] R. J. Van Brunt, "Production Rates for Oxyfluorides SOF_2, SO_2F_2, and SOF_4 in SF_6 Corona Discharges", J. Res. Nat. Bur. Stand., Vol. 90, pp. 229–253, 1985.

[16] F. Y. Chu, "SF_6 Decomposition in Gas-insulated Equipment", IEEE Trans. Elec. Insul., Vol. 21, pp. 693–726, 1986.

[17] H. Slowikowska, T. Las,, J. Slowikowski and R. J. Van brunt, "Modification of Cast Epoxy Resin, Surfaces During Exposure to Partial Discharge", Proc. 7th Int. Symp. on Gaseous Dielectrics, Plenum, NY (in press, 1994)

[18] R. J. Van Brunt, P. von Glahn and T. Las, "Nonstationary Behavior of Partial Discharge During Discharge-induced Aging of Dielectrics", IEE Proc. -Sci., Meas., Tech., (in press, 1994).

[19] C. Hudon, R. Bartnikas and M. R. Wertheimer, "Spark-to-glow Discharge Transition Due to Increased Surface Conductivity on Epoxy Resin Specimens", IEEE Trans. Elec. Insul., Vol. 28, pp. 1–8, 1993.

[20] N. Foulon-Belkacemi, M. -P. Panaget, M. Goldman and A. Goldman, "Influence of Electrode Materials and Coverings on the Gaseous By-products Generated by Air Corona Discharges", Proc. 7th Int. Symp. on Gaseous Dielectrics, Plenum, NY (in press, 1994)

[21] J. P. Borra, A. Goldman and M. Goldman, "Generation of Condensation Nuclei by dc Electrical Discharges in Point-to-plane Configuration", J. Aerosol Sci. (in press, 1994).

[22] C. Hudon, R. Bartnikas and M. R. Wertheimer, "Analysis of Degradation Products on Epoxy Surfaces Subjected to Pulse and Glow-type Discharge", 1991 Annual Report-Conference on Electrical Insulation and Dielectric Phenomena, IEEE, NY, pp. 237–243, 1991.

[23] T. Okamoto and T. Tanaka, "Prediction of Treeing Breakdown from Pulse Height of Partial Discharge on Voltage-phase Angle", Japanese J. Appl. Phys., Vol. 24, pp. 156–160, 1985.

[24] J. T. Holboll and M. Henriksen, "Partial Discharge Patterns Related to Surface Deterioration in Voids in Epoxy", Conf. Record - 1990 IEEE Int. Symp. on Elec. Insul., IEEE publ. CH2727- 6/90, pp. 115–119, 1990.

[25] T. Ito, K. Jogan, T. Saito and Y. Ehara, "Phase Analysis of Discharge Magnitude Distributions Inside a Small Void and Its Application to Diagnosis of Deteriorating Insulations", 1989 Annual Report - Conference on Electrical Insulation and Dielectric Phenomena, IEEE, NY, pp. 111–116, 1989.

[26] F. Komori, N. Nishiguchi, M. Hikita and T. Mizutani, "Detection of Electrical Tree Initiation and Assessment of Shape of the Developing Tree Using Pattern Recognition of Partial Discharge Occurrence Phase Distribution", IEE Conference Proceedings No. 378, pp. 68–69, 1993; "Construction of Expert System Prototype for Degradation Diagnosis and Measurement System Using Personal Computer: Application for Degradation Diagnosis of PD Statistical Parameter Using Phase Information", Trans. IEE Japan, Vol. 113-A, pp. 406–415, 1993.

[27] R. J. Van Brunt, P. von Glahn and T. Las, "Partial Discharge-induced Aging of Cast Epoxies and Related Nonstationary Behavior of the Discharge Statistics", 1993 Annual Report - Conference on Electrical Insulation and Dielectric Phenomena, IEEE, NY, pp. 455–461, 1993.

[28] R. J. Van Brunt, "Stochastic Properties of Partial-discharge Phenomena", IEEE Trans. Elec. Insul., Vol. 26, pp. 902–948, 1991.

[29] R. Bartnikas, "Detection of Partial Discharges (Corona) in Electrical Apparatus", IEEE Trans. Elec. Insul., Vol. 25, pp. 111–123, 1990.

[30] R. S. Sigmond, "Corona Discharges", in *Electrical Breakdown in Gases*, ed. J. M. Meek and J. D. Craggs, John Wiley and Sons, New York, pp. 319–384, 1978.

[31] M. Goldman and A. Goldman, "Corona Discharges", in *Gaseous Electronics*, Vol. 1, Academic Press, NY, pp. 219–290, 1978.

[32] J. H. Mason, "Discharges", IEEE Trans. Elec. Insul., Vol. 13, pp. 211–238, 1978.

[33] J. C. Devins, "The Physics of Partial Discharges in Solid Dielectrics", IEEE Trans. Elec. Insul., Vol. 19, pp. 475–495, 1984.

[34] R. Bartnikas, "A Commentary on Partial Discharge Measurement and Detection", IEEE Trans. Elec. Insul., Vol. 22, pp. 629–633, 1987.

[35] A. Pedersen, "On the Electrical Breakdown of Gaseous Dielectrics", IEEE Trans. Elec. Insul., Vol. 24, pp. 721–739, 1989.

[36] G. W. Trichel, "Mechanism of the Negative Point-to-plane Corona Near Onset", Phys. Rev., Vol. 54, pp. 1078–1084, 1938.

[37] M. Cernak and T. Hosokawa, "Initial Stages of Negative Point-to-plane Breakdown in Helium", Japanese J. Appl. Phys., Vol. 26, pp. L1721–L1723, 1987.

[38] R. J. Van Brunt and M. Misakian, "Mechanisms for Inception of dc and 60-Hz AC Corona in SF_6", IEEE Trans. Elec. Insul., Vol. 17, pp. 106–120, 1982.

[39] B. Eliasson and V. Kogelschatz, "Modeling and Applications of Silent Discharge Plasmas", IEEE Trans. Plasma Sci., Vol. 19, pp. 309–323, 1991.

[40] R. Bartnikas and J. P. Novak, "On the Spark to Pseudoglow and Glow Transition Mechanism and Discharge Detectability", IEEE Trans. Elec. Insul., Vol. 27, pp. 3–14, 1992.

[41] M. G. Danikas, R. Bartnikas and J. P. Novak, "Discussion-on the Spark to Pseudoglow and Glow Transition Mechanism and Discharge Detectability", IEEE Trans. Elec. Insul., Vol. 28, pp. 429–431, 1993.

[42] Y. Kondo and Y. Miyoshi, "Pulseless Corona in Negative Point to Plane Gap", Japanese J. Appl. Phys., Vol. 17, pp. 643–649, 1978.

[43] D. B. Ogle and G. A. Woolsey, "Current Pulses in SF_6 Glow Discharges", J. Phys. D: Appl. Phys., Vol. 22, pp. 1829–1834, 1989.

[44] T. Ishida, Y. Mizumo, N. Nagao and M. Kosaki, "Computer Aided Partial Discharge Analyzing System for Detection of Swarming Pulsive Microdischarges", IEE Conference Proceedings No. 378, pp. 99–100, 1993.

[45] S. K. Dhali and P. F. Williams, "Two-dimensional Studies of Streamers in Gases", J. Appl. Phys., Vol. 62, pp. 4696–4707, 1987.

[46] J. Liu and G. R. Govinda Raju, "Streamer Formation and Monte-Carlo Space-charge Field Calculation in SF_6", IEEE Trans. Elec. Insul., Vol. 28, pp. 261–270, 1993.

[47] R. J. Van Brunt and J. T. Herron, "Fundamental Process of SF_6 Decomposition and Oxidation in Glow and Corona Discharges", IEEE Trans. Elec. Insul., Vol. 25, pp. 75–94, 1990.

[75] N. Hozumi, T. Okamoto and H. Fukagawa, "Simultaneous Measurement of Microscopic Image and Discharge Pulses at the Moment of Electrical Tree Initiation", Japanese J. Appl. Phys., Vol. 27, pp. 572–576, 1988.

[76] R. J. Van Brunt, E. W. Cernyar, P. von Glahn and T. Las, "Variations in the Stochastic Behavior of Partial-discharge Pulses with Point-to-dielectric Gap Spacing", Conf. Record-1992 IEEE Int. Symp. on Elec. Insul., IEEE publ. 92 CH3150–0, pp. 349–353, 1992.

[77] E. C. Rogers, "The Self-extinction of Gaseous Discharges in Cavities in Dielectrics", Proc. IEE, Vol. 104 A, pp. 621–630, 1958.

[78] P. von Glahn and R. J. Van Brunt, "Performance Evaluation of a New Digital Partial Discharge Recording and Analysis System", Conf. Record-1994 IEEE Int. Symp. on Elec. Insul., IEEE publ. 94 CH3445–4, pp. 12–16, 1994.

[79] R. J. Van Brunt and D. A. Leep, "Corona-induced Decomposition of SF_6", *Gaseous Dielectrics III*, Proc. 3rd Int. Symp. on Gaseous Dielectrics, ed. L. G. Christophorou, Pergamon Press, NY, pp. 402–409, 1982.

[80] R. J. Van Brunt and D. A. Leep, "Characterization of Point-plane Corona Pulses in SF_6", J. Appl. Phys., Vol. 52, pp. 6588–6600, 1981.

[81] R. J. Van Brunt, "Effects of H_2O on the Behavior of SF_6 Corona", Proc. 7th Int. Conf. on Gas Discharges and Their Applications, Peter Peregrinas, pp. 255–258, 1982.

[82] R. J. Van Brunt, "Water Vapor-enhanced Electron-avalanche Growth in SF_6 for Nonuniform Fields", J. Appl. Phys., Vol. 59, pp. 2314–2323, 1986.

[83] J. K. Olthoff, R. J. Van Brunt, Y. Wang, R. L. Champion and L. D. Doverspike, "Collisional Electron Detachment and Decomposition Rates of SF_6^-, SF_5^-, and F^- in SF_6: Implications for Ion Transport and Electrical Discharges", J. Chem. Phys., Vol. 91, pp. 2261–2268, 1989.

[84] I. Sauers and G. Harman, "A Mass Spectometric Study of Positive and Negative Ion Formation in an SF_6 Corona. Part II: Influence of Water and SF_6 Neutral By-products", J. Phys. D: Appl. Phys., Vol. 25, pp. 774–782, 1992.

[85] E. Gulski and A. Krivda, "Neural Networks as a Tool for Recognition of Partial Discharges", IEEE Trans. Elec. Insul., Vol. 28, pp. 984–1001, 1993.

[86] N. Hozumi, T. Okamoto and T. Imajo, "Discrimination of Partial Discharge Patterns Using a Neural Network", IEEE Trans. Elec. Insul., Vol. 27, pp. 550–555, 1992.

[87] A. A. Mazroua, R. Bartnikas and M. M. A. Salama, "Discrimination Between PD Pulse Shapes Using Different Neural Network Paradigms", IEEE Trans. Diel. Elec. Insul. (in press, 1994)

[88] M. Piemontesi, R. Pietsch and W. Zaengl, "Analysis of Decomposition Products of Sulfur Hexafluoride in Negative dc Corona with Special Emphasis on Content of H_2O and O_2", Conf. Record-1994 IEEE Int. Symp. on Elec. Insul., IEEE publ. 94 CH3445–4, pp. 499–503, 1994.

[89] A. M. Casanovas, J. Casanovas, F. Lagerde and A. Belarbi, "Study of the Decomposition of SF_6 under the Negative Polarity Corona Discharge (Point-to-plane Geometry): Influence of the Metal Constituting the Plane Electrode", J. Appl. Phys., Vol. 72, pp. 3344–3354, 1992.

[90] R. J. Van Brunt, J. K. Olthoff and M. Shah, "Rate of S_2F_{10} Production from Negative Corona in Compressed SF_6", Conf. Record-1992 IEEE Int. Symp. on Elec. Insul., IEEE publ. 92 CH3150–0, pp. 328–331, 1992.

[91] M. C. Siddagangappa, R. J. Van Brunt and A. V. Phelps, "Influence of Oxygen on the Decomposition Rate of SF_6 in Corona", Conf. Record-1986 IEEE Int. Symp. on Elec. Insul., IEEE publ. 86 CH2196–4-DEI, pp. 225–229, 1986.

[92] J. B. Whitehead, "The Electric Strength of Air", Trans. AIEE, Vol. 29, pp. 1159–1187, 1910; "The Electric Strength of Air II", Trans. AIEE, Vol. 30, pp. 1857–1965, 1911.

Manuscript was received on 22 July 1994.